Table 3 Possible measures to promote the involvement of general practitioners (GPs) in palliative care

1) Training and seminars
   - Seminars or conferences at which GPs and hospital specialists can discuss the appropriate timing of discharge are necessary.
   - I want to learn the necessary skills to carry out procedures like continuous subcutaneous injection of opioids and nephrostomy.
   - I think I would be able to deal with such procedures as continuous subcutaneous injection and nephrostomy if I were trained; I just happen not to have received training.
   - Doctors with different specialties focus on different issues, so seminars that can bring all the specialties together need to be organized.
   - I would like to attend seminars on useful procedures such as IVH and continuous subcutaneous injection.
   - Training is needed for all professionals, including home care nurses and care givers.

2) Good relationships between hospital doctors and GPs
   - I want to enter into detailed discussion with hospital specialists as soon as the patient is diagnosed.
   - Time is needed to build up a relationship with a patient, so hospitals should provide more information in advance of the patient's discharge.
   - Networks are needed to establish close relationships between GPs and hospital specialists.
   - Hospitals providing cancer treatment and GPs should collaborate to provide good care.
   - Besides a reply to my referral letter, I want to know details about the progress of my patients after operations or treatment in the hospital.

3) Support from hospital palliative care team
   - The core hospital should be ready to treat any patient who needs emergency pain control at any time.
   - The core hospital and the 3 other hospitals in this area should cooperate to support patients according to the stage of their disease and symptoms.
   - The first step is to establish a system which enables hospitals to discharge their patients so that they can receive care at home, and the second step is to establish a back-up system for emergencies.

4) Group practice
   - It is impossible for one doctor to be available 24 hours a day. Three doctors working as a group can take care of more patients, but there are very few doctors who are prepared to cover nights.
   - Group practice widens the range of care and treatment that can be provided.
   - I think group practice and medical networks are effective, but my clinic is a long way from the city.
   - Group practice requires trusting relationships among member doctors. We need to establish a system of group practice as the norm.

5) Education of patients, families and citizens
   - Whether the family is ready to deal with it is the key to whether a patient can die at home.
   - Some families prefer to communicate only with hospital doctors. Patients and their families need to be better educated about medical services.
   - Education about health and disease prevention is also important in this area.
   - Citizens need to be engaged in frank discussions about life and death.
   - It may take a long ted to change citizens' perceptions of and attitudes toward home care.

J Pharmacol Sci 112, 424 – 431 (2010)

Journal of Pharmacological Sciences

Full Paper

Analysis of the Effects of Anesthetics and Ethanol on μ-Opioid Receptor

Kouichiro Minami[1,3,*], Yuka Sudo[2,3], Seiji Shiraishi[3], Masanori Seo[1], and Yasuhito Uezono[3]

[1]*Department of Anesthesiology and Critical Care Medicine, Jichi Medical University, Tochigi 329-0483, Japan*
[2]*Department of Molecular and Cellular Biology, Nagasaki University School of Biomedical Sciences, Nagasaki 852-8523, Japan*
[3]*Cancer Pathophysiology Division, National Cancer Center Research Institute, Tokyo 104-0045, Japan*

Received January 6, 2010; Accepted February 15, 2010

Abstract. G protein–coupled receptors, in particular, Ca^{2+}-mobilizing G_q-coupled receptors have been reported to be targets for anesthetics. Opioids are commonly used analgesics in clinical practice, but the effects of anesthetics on the opioid μ-receptors (μOR) have not been systematically examined. We report here an electrophysiological assay to analyze the effects of anesthetics and ethanol on the functions of μOR in *Xenopus* oocytes expressing a μOR fused to chimeric Gα protein G_{qi5} (μOR-G_{qi5}). Using this system, the effects of halothane, ketamine, propofol, and ethanol on the μOR functions were analyzed. In oocytes expressing μOR-G_{qi5}, the μOR agonist DAMGO ([D-Ala^2,*N*-MePhe^4,Gly-ol]-enkephalin) elicited Ca^{2+}-activated Cl^- currents in a concentration-dependent manner (EC_{50} = 0.24 μM). Ketamine, propofol, halothane, and ethanol themselves did not elicit any currents in oocytes expressing μOR-G_{qi5}, whereas ketamine and ethanol inhibited the DAMGO-induced Cl^- currents at clinically equivalent concentrations. Propofol and halothane inhibited the DAMGO-induced currents only at higher concentrations. These findings suggest that ketamine and ethanol may inhibit μOR functions in clinical practice. We propose that the electrophysiological assay in *Xenopus* oocytes expressing μOR-G_{qi5} would be useful for analyzing the effects of anesthetics and analgesics on opioid receptor function.

Keywords: μ-opioid receptor, $G_{i/o}$-coupled receptor, ketamine, ethanol, *Xenopus* oocyte

Introduction

Opioids are commonly used analgesics in clinical practice, but the role of opioid receptor (OR) in anesthetic action has still been unclear. It has been reported that the OR antagonist naloxone does not affect the anesthetic potency of volatile anesthetics halothane in animals (1, 2). On the other hand, Sarton et al. reported that S(+) ketamine interacts with the μ-opioid system at supraspinal sites (3). In order to clarify the role of ORs in anesthetic action, it would be necessary to study the direct effects on OR function.

Several lines of studies have been reported that metabotropic G protein–coupled receptors (GPCRs) are now recognized as targets for anesthetics and analgesics (4). We and others have previously reported that functions of G_q protein–coupled receptors, including muscarinic type1 receptors (M_1R) (5), metabotropic type 5 glutamate receptors (mGluR5) (6), 5-hydroxytryptamine (5HT) type 2A receptors (7), and substance P receptors (8), are inhibited by anesthetics and analgesics. The ORs belong to the GPCR family and three types of ORs, μ, δ, and κ, have been identified by molecular cloning (9). Within three subtypes of these receptors, μORs are the major receptor to mediate the analgesic effects of opioids (9). On the basis of second messenger signaling, μOR couple to $G\alpha_{i/o}$ protein to cause inhibition of adenylate cyclase, inhibition of voltage-dependent Ca^{2+} channels, or activation of G protein–coupled inwardly rectifying K^+ channels (GIRKs) (9). Functions of G_q-coupled receptors have been reported to be modified by some anesthetics and analgesics (4, 10); as far as the functions of $G_{i/o}$-coupled receptors including μOR are concerned, much less is known about the direct effects of anesthetics and analgesics.

The *Xenopus* oocyte expression system has widely

*Corresponding author. kminami@med.uoeh-u.ac.jp
Published online in J-STAGE on April 2, 2010 (in advance)
doi: 10.1254/jphs.10003FP

been employed to study functions of a number of GPCRs (4, 10). In the case of G_q-coupled receptors, stimulation of the receptors result in activation of Ca^{2+}-activated Cl^- currents in *Xenopus* oocytes by G_q-mediated activation of phospholipase C (PLC) and subsequent formation of IP_3 and diacylglycerol (4, 11). The IP_3 formed causes release of Ca^{2+} from the endoplasmic reticulum by activation of IP_3 receptors (IP_3R), which in turn, triggers the opening of Ca^{2+}-activated Cl^- channels endogenously expressed in the oocytes (4, 11). However, in the case of $G_{i/o}$-coupled receptors, analysis has been difficult due to lack of appropriate analytical output in oocytes. We have established the assay method for $G_{i/o}$-coupled receptors by using G_{qi5} chimeric G protein to switch the $G_{i/o}$ signal to a G_q signal (12). By using this assay system, we reported that halothane inhibited the function of $G_{i/o}$-coupled muscarinic M_2 receptor (M_2R) in oocytes coexpressing M_2R and G_{qi5} (13). Recently, in order to improve the $G_{i/o}$-coupled–receptor assay system, we made a μOR fused to G_{qi5} (μOR-G_{qi5}) and expressed it in *Xenopus* oocytes (13).

By using this assay system, we examined the effects of halothane, ketamine, propofol, and ethanol on the function of μOR.

Materials and Methods

Materials

Adult *Xenopus laevis* female frogs were purchased from Kato Kagaku (Tokyo); halothane, from Dinabot Laboratories (Osaka), and the Ultracomp *E. coli* Transformation Kit, from Invitrogen (San Diego, CA, USA). Purification of cDNAs was performed with a Qiagen purification kit (Qiagen, Chatworth, CA, USA). Gentamicin, sodium pyruvate, [D-Ala^2,*N*-MePhe^4,Gly-ol]-enkephalin (DAMGO), and propofol were purchased from Tokyo Kagaku (Tokyo), and ketamine was purchased from Sigma (St. Louis, MO, USA). Other chemicals are analytical grade and were from Nacalai Tesque (Kyoto). The rat μOR was provided by Dr. N. Dascal (Tel Aviv University, Ramat Aviv, Israel). The chimeric $G\alpha_{qi5}$ was a kind gift from Dr. B.R. Conklin (The University of California, San Francisco, CA, USA). Each of the cRNAs was prepared by using an mCAP mRNA Capping Kit and transcribed with a T7 RNA Polymerase in vitro Transcription Kit (Stratagene, La Jolla, CA, USA).

Preperartion of chimeric μOR-Gqi5

The tandem cDNAs of chimeric μOR-G_{qi5} was created by ligating the receptor cDNA sequences into the NheI site of G_{qi5} cDNAs. The sequences of all PCR products were confirmed by sequencing with ABI3100 (Applied BioSystems, Tokyo). All cDNAs for the synthesis of cRNAs were subcloned into the pGEMHJ vector, which provides the 5′- and 3′-untranslated region of the *Xenopus* β-globin RNA (14), ensuring a high level of protein expression in the oocytes. Each of the cRNAs was synthesized using the mCAP mRNA Capping Kit, with the T7 RNA polymerase in vitro Transcription Kit (Ambion, Austin, TX, USA) from the respective linearized cDNAs.

Recording and data analyses

Isolation and microinjection of *Xenopus* oocytes were performed as previously described (12, 13). *Xenopus* oocytes were injected with appropriate amounts of cRNAs (50 ng, μOR-G_{qi5}) and incubated with ND 96 medium composed of 96 mM NaCl, 2 mM KCl, 1.8 mM $CaCl_2$, 1 mM $MgCl_2$, 5 mM HEPES (pH 7.4, adjusted with NaOH), supplemented with 2.5 mM sodium pyruvate and 50 μg/ml gentamicin for 3 – 7 days until recording. Oocytes were placed in a 100-ml recording chamber and perfused with MBS (modified Barth's saline) composed of 88 mM NaCl, 1 mM KCl, 2.4 mM $NaHCO_3$, 10 mM HEPES, 0.82 mM $MgSO_4$, 0.33 mM $Ca(NO_3)_2$, and 0.91 mM $CaCl_2$, (pH 7.4 adjusted with NaOH) at a rate of 1.8 ml/min at room temperature. Recording and clamping electrodes (1 – 2 MΩ) were pulled from 1.2-mm outside diameter capillary tubing and filled with 3 M KCl. A recording electrode was imbedded in the animal's pole of oocytes, and once the resting membrane potential stabilized, a clamping electrode was inserted and the resting membrane potential was allowed to restabilize. A Warner OC 725-B oocyte clamp (Hampden, CT, USA) was used to voltage-clamp each oocyte at −70 mV. We analyzed the peak component of the transient inward currents induced by receptor agonists because this component is dependent on the concentrations of the receptor agonist applied and is quite reproducible, as described by Minami et al. (15). Anesthetics (halothane, ketamine, propofol) and ethanol were applied for 2 min before and during the application of test compounds to allow complete equilibration in the bath. The solutions of halothane were freshly prepared immediately before use. We calculated the final concentration of halothane in the recording chamber as reported previously (16), and accordingly, the concentrations of halothane represent the bath concentrations.

Statistical analyses

Results are expressed as percentages of control responses. The control responses were measured before and after each drug application, to take into account possible shifts in the control currents as recording proceeded. The "n" values refer to the number of oocytes studied. Each experiment was carried out with oocytes from at

least two different frogs. Statistical analyses were performed using a one-way ANOVA (analysis of variance) and the Dunnet correction. Curve fitting and estimation of EC_{50} values for the concentration–response curves were performed using Graphpad Inplot Software (San Diego, CA, USA).

Results

DAMGO-induced Ca^{2+}-activated Cl^- currents in Xenopus oocytes expressing $\mu OR\text{-}G_{qi5}$

We first determined the effects of the μOR agonist DAMGO on the Ca^{2+}-activated Cl^- currents in *Xenopus* oocytes expressing μOR-G_{qi5}. As shown in Fig. 1A, DAMGO at 0.1 μM elicited a robust Ca^{2+}-activated Cl^- current. There were no Cl^--currents in oocytes expressing μOR not fused to G_{qi5} even at 10 μM DAMGO (data not shown), as reported previously (13). The EC_{50} of the DAMGO-induced Cl^- currents was 0.24 ± 0.01 μM (Fig. 1B).

Analysis of ketamine and propofol on DAMGO-induced Ca^{2+}-activated Cl^- currents in Xenopus oocytes expressing $\mu OR\text{-}G_{qi5}$

By using this assay, we examined the effects of the intravenous anesthetic ketamine on the μOR function in *Xenopus* oocytes expressing μOR-G_{qi5}. Ketamine by itself did not elicit any currents in oocytes expressing μOR-G_{qi5} but significantly inhibited DAMGO-induced Ca^{2+}-activated Cl^- currents in a concentration-dependent manner (Fig. 2A). Ketamine at 0.1, 1, and 10 μM inhibited the

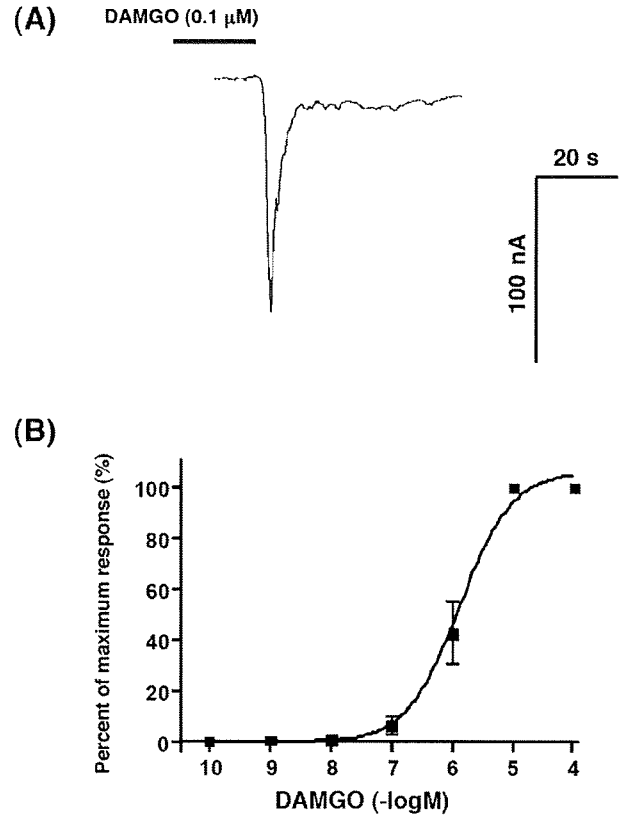

Fig. 1. Electrophysiological μOR assay induced by the μOR agonist DAMGO in *Xenopus* oocytes expressing μOR-G_{qi5}. A: Typical tracing of DAMGO (0.1 μM)-induced Ca^{2+}-activaed Cl^- current in an oocyte expressing μOR-G_{qi5}. B: Concentration–response curves of DAMGO-induced Ca^{2+}-activated Cl^- currents in oocytes. Oocytes were voltage-clamped at −70 mV and DAMGO was applied for 20 s.

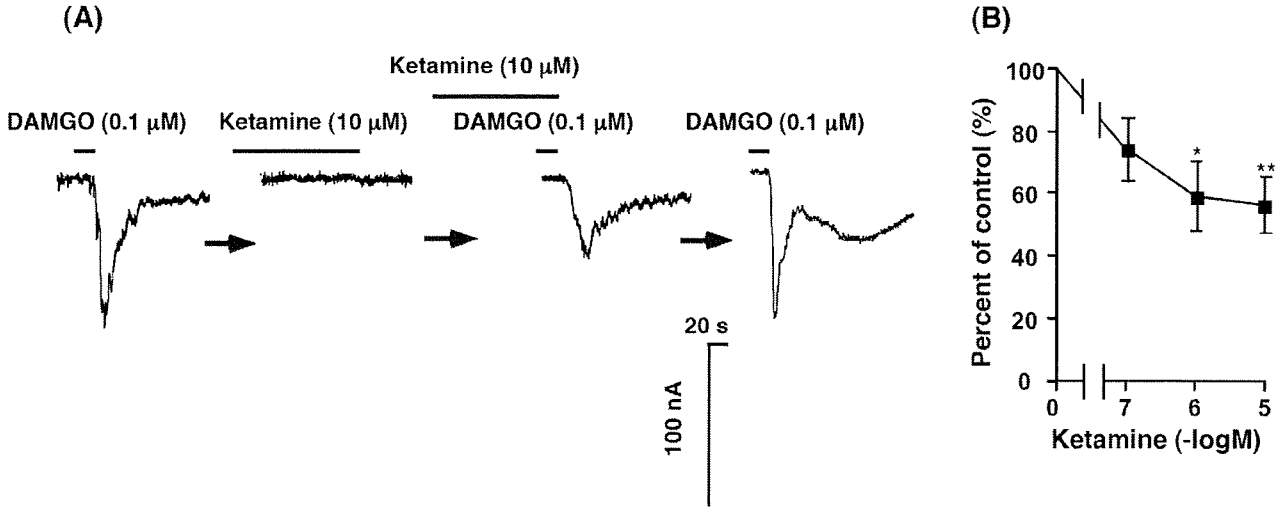

Fig. 2. Effects of ketamine on the basal and DAMGO-induced Ca^{2+}-activated Cl^- currents in oocytes expressing μOR-G_{qi5}. A: Typical tracings of the effect of 10 μM ketamine on the Cl^- current evoked by 0.1 μM DAMGO in an oocyte expressing μOR-G_{qi5}. B: Concentration–response curve for the inhibitory effects of ketamine on DAMGO (0.1 μM)-induced Cl^- currents in oocytes expressing μOR-G_{qi5}. $^*P < 0.05$ and $^{**}P < 0.01$ vs. control.

DAMGO-induced Cl^- currents to 74 ± 10.3%, 59.1 ± 11.3%, and 56.2 ± 9.3% of the control value, respectively (n = 6 for each) (Fig. 2B).

We next determined the effects of another intravenous anesthetic propofol on the function of μOR in oocytes expressing μOR-G_{qi5} (Fig. 3). Propofol by itself elicited no currents, but inhibited DAMGO-induced Cl^- currents in oocytes expressing μOR-G_{qi5} in a concentration-dependent manner (Fig. 3A). Propofol at concentrations of 0.1, 1, 10, and 100 μM inhibited the DAMGO-induced Cl^- currents to 93.3 ± 3.7%, 73.5 ± 7.9%, 72.8 ± 5.7%, and 53.7 ± 7.5% of the control value, respectively (n = 6 for each) (Fig. 3B).

Analysis of halothane and ethanol on the DAMGO-induced Ca^{2+}-activated Cl^- currents in Xenopus oocytes expressing μOR-G_{qi5}

We then examined the effects of the volatile anesthetic halothane on the function of μOR in oocytes expressing μOR-G_{qi5} (Fig. 4). Halothane by itself did not elicit any currents in oocytes expressing μOR-G_{qi5} at concentrations up to 2 mM, (Fig. 4A). Higher concentrations of halothane more than 1 minimum alveolar concentration (MAC, 0.25 mM) had inhibitory effects on the DAMGO-induced Cl^- currents in a concentration-dependent manner; 1MAC concentration of halothane did not suppress DAMGO-induced Cl^- currents. Halothane at concentrations of 0.25, 0.5, 1, and 2 mM inhibited the current to 75.1 ± 12.4%, 57.8 ± 10.3%, 54.7 ± 10.3%, and 48.6 ± 9.4% of the control value, respectively (n = 6 for each) (Fig. 4B).

We finally examined the effects of ethanol on the function of μOR in oocytes expressing μOR-G_{qi5} (Fig. 5). Ethanol by itself had no effects in oocytes expressing μOR-G_{qi5}, but it significantly inhibited DAMGO-induced Cl^- currents in a concentration-dependent manner (Fig. 5B). Ethanol at concentrations of 25, 50, 100, and 200 mM inhibited the currents to 53.1 ± 10.1%, 47 ± 13.3%, 43.3 ± 9.6%, and 35 ± 5.3% of the control value, respectively (n = 6 for each) (Fig. 5B).

Discussion

We previously proposed an electrophysiological assay of the $G_{i/o}$-coupled receptors in *Xenopus* oocytes expressing the receptors and chimeric G protein G_{qi5} (12, 13). By using this system, we examined the effects of several anesthetics and ethanol on the μOR function in oocytes expressing fused μOR-G_{qi5}.

In general, $G_{i/o}$-coupled receptors such as μOR are known to inhibit adenylate cyclase to decrease cAMP levels in the cells (9). Numerous reports have shown that ketamine, halothane, and ethanol increase basal cAMP levels in a variety of the cells, possibly by direct activation of adenylate cyclases (17 – 20); thus it might be difficult to estimate the effects of anesthetics and ethanol

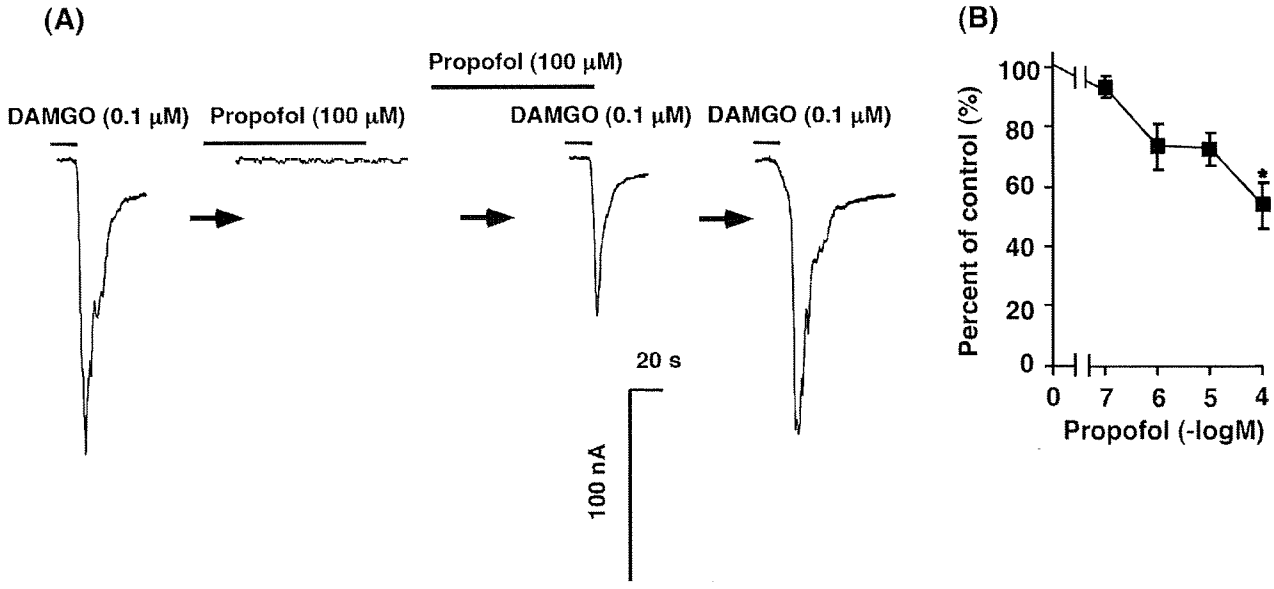

Fig. 3. Effects of propofol on the basal and DAMGO-induced Ca^{2+}-activated Cl^- currents in oocytes expressing μOR-G_{qi5}. A: Typical tracings of the effect of 100 μM propofol on the Cl^- current evoked by 0.1 μM DAMGO in an oocyte expressing μOR-G_{qi5}. B: Concentration–response curve for the inhibitory effects of propofol on DAMGO (0.1 μM)–induced Cl^- currents in oocytes expressing μOR-G_{qi5} *$P < 0.05$ and vs. control.

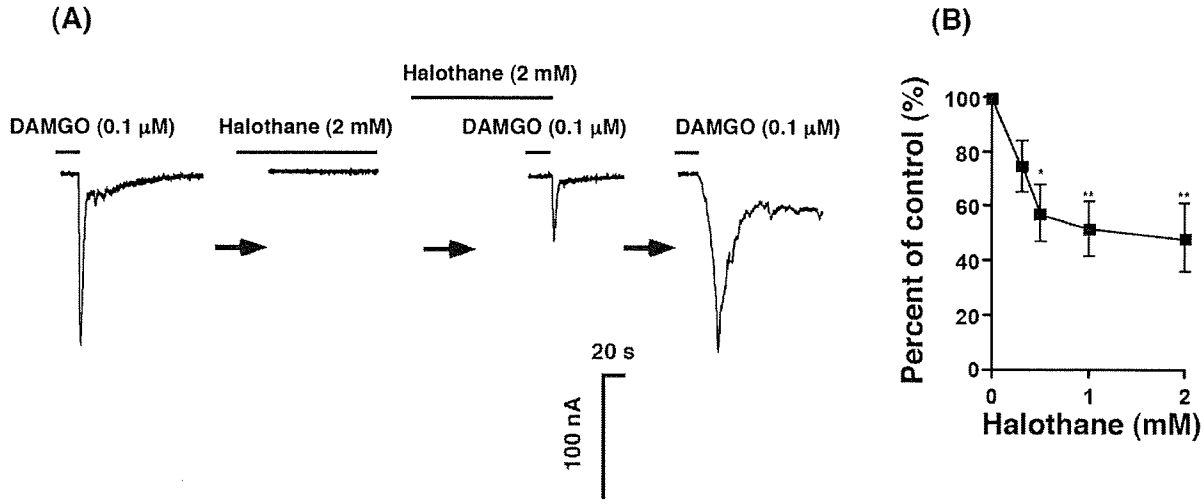

Fig. 4. Effects of halothane on the basal and DAMGO-induced Ca^{2+}-activated Cl^- currents in oocytes expressing μOR-G_{qi5}. A: Typical tracings of the effect of 2 mM halothane on the Cl^- current evoked by 0.1 μM DAMGO in an oocyte expressing μOR-G_{qi5}. B: Concentration–response curve for the inhibitory effects of halothane on DAMGO (0.1 μM)–induced Cl^- currents in oocytes expressing μOR-G_{qi5}. $^*P < 0.05$ and $^{**}P < 0.01$ vs. control.

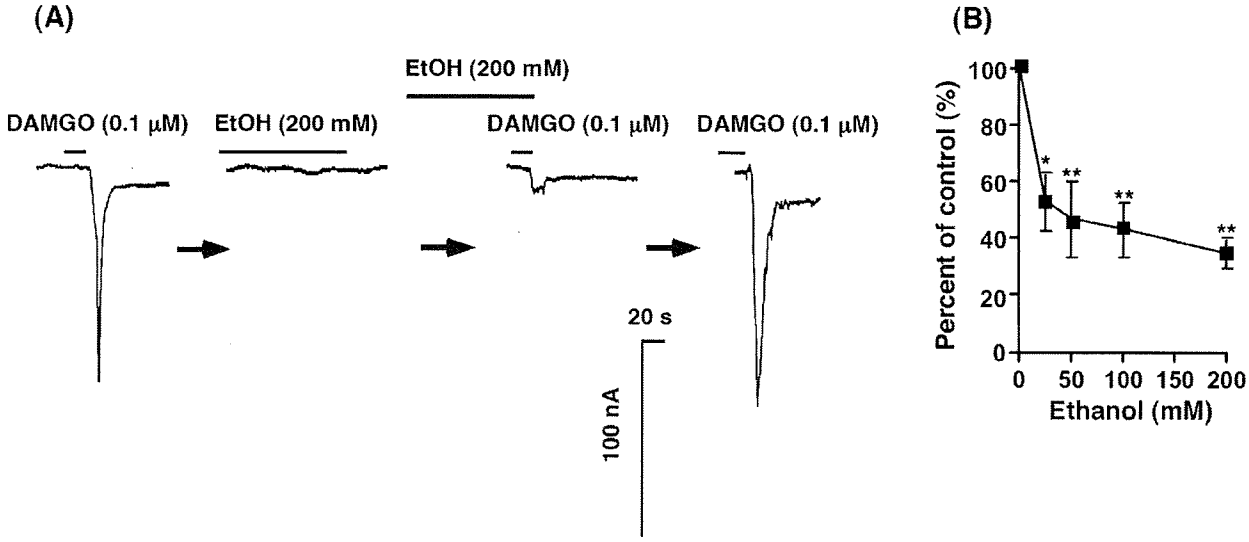

Fig. 5. Effects of ethanol on the basal and DAMGO-induced Ca^{2+}-activated Cl^- currents in oocytes expressing μOR-G_{qi5}. A: Typical tracings of the effect of 200 mM ethanol on the Cl^- current evoked by 0.1 μM DAMGO in an oocyte expressing μOR-G_{qi5}. B: Concentration–response curve for the inhibitory effects of ethanol on DAMGO (0.1 μM)–induced Cl^- currents in oocytes expressing μOR-G_{qi5}. $^*P < 0.05$ and $^{**}P < 0.01$ vs. control.

on the functions of $G_{i/o}$-coupled receptors by using a cAMP inhibition assay. Alternatively we and others have used *Xenopus* oocytes expressing GIRK channels for the analysis of functions of $G_{i/o}$-coupled receptors such as μOR, $GABA_BR$, or cannabinoid CB_1 and CB_2 receptors (13, 21 – 23); GIRKs have been demonstrated to be excellent reporter channels for assay of the activity of $G_{i/o}$-coupled receptors (21). However, recent reports have revealed that GIRKs are possible targets for several anesthetics including halothane and ethanol (24 – 26). In such a situation, it should be taken into consideration that functions of either $G_{i/o}$-coupled receptors, GIRKs, or both could be affected by anesthetics or alcohol if GIRKs are used as reporters (24 – 26). In this study, we thus employed μOR-G_{qi5} in a *Xenopus* oocyte expression assay system. Accordingly, this system makes it possible

to study the direct effects of anesthetics and alcohols on μOR functions.

In the present study, we demonstrated that ketamine and ethanol inhibited the DAMGO-induced Cl^- currents at clinically equivalent concentrations, while propofol and halothane inhibited the DAMGO-induced currents only at higher concentrations. In our experimental system, the inhibitory effects of the anesthetics and ethanol are considered due to specific inhibition of μOR or the inhibition of the downstream steps in the μOR-induced G_{qi5}–PLC–IP_3–IP_3R–Ca^{2+} mobilization pathways. There are numerous reports showing that ketamine, propofol, halothane, and ethanol did not inhibit such downstream pathways after activation of GPCRs in the *Xenopus* oocyte expression system. In the case of ketamine and halothane, they inhibit muscarinic M_1R-mediated Ca^{2+}-activated Cl^- currents in clinically relevant concentrations (5, 27) without affecting angiotensin II receptor (AT_1R)–induced Cl^- currents, although activation of M_1R and AT_1R consequently activate the same G_q–PLC–IP_3–IP_3R–Ca^{2+} mobilization pathways (5, 27). These results suggest that ketamine and halothane affect functions of Ca^{2+}-mobilizing GPCRs possibly by receptor sites rather than the downstream pathway after GPCR activation. As for propofol, our previous study demonstrated that this anesthetic inhibited the functions of M_1R but not substance P receptors, although both receptors were considered to couple to the same Gq-mediated pathways (8, 28). In addition, we demonstrated that propofol (50 μM) did not inhibit the direct G protein activator AlF_4^-–induced Ca^{2+}-activated Cl^- currents in *Xenopus* oocytes (28). In the case of ethanol, we previously reported that ethanol also selectively inhibited the glutamate mGluR5 but not mGluR1, although both receptors couple to Gq to activate Ca^{2+}-activated Cl^- currents in oocytes (6). Taken together, these findings indicate that anesthetics and ethanol employed in the present study may not inhibit the step of G protein–PLC–IP_3–IP_3R–Ca^{2+} mobilization in the μOR signaling pathway.

The EC_{50} value of DAMGO of the μOR-induced Ca^{2+}-activated Cl^--currents through G_{qi5} was 0.24 μM in the present study. In our previous experimental study in *Xenopus* oocytes expressing μOR-G_{qi5} (13), the EC_{50} of DAMGO was approximately 0.1 μM. In *Xenopus* oocytes expressing cloned μOR and GIRKs, the EC_{50} values of DAMGO were 0.1 (13), 0.034 – 0.133 (29), and 0.02 – 0.09 μM (30) determined with the GIRK channel assay. These results suggest that our present EC_{50} value seems not too far from the previously reported EC_{50} values obtained in *Xenopus* oocytes expressing μOR.

We showed that ketamine had an inhibitory effect on DAMGO-induced Cl^- currents in oocytes expressing μOR-G_{qi5} at concentrations more than 1 μM. In clinical situations, the free plasma concentration of ketamine was approximately 10.5 – 60 μM (31, 32). Previous reports showed that higher concentration of ketamine than those in clinical usage (50 – 100 μM) displaced [^{3}H]diprenorphine binding to μORs expressed in Chinese hamster ovary cells (33). In an animal study, S(+)ketamine interacts with the μOR, which contributed to S(+)ketamine-induced respiratory depression and supraspinal antinociception (3). Consistent with these reports, our present results suggest that anesthetic concentrations of ketamine would have direct inhibitory effects on μOR.

The effects of propofol on the μOR functions have not been reported so far. In the present study, only high concentration (100 μM) of propofol (but less than 100 μM) had inhibitory effects on the DAMGO-induced Cl^- currents in oocytes expressing μOR-G_{qi5}. In humans, the peak plasma concentration of propofol after intravenous injection of the anesthetic dosage of 2.5 mg/kg was approximately 23 ± 0.24 μM (34). From our present results, it seems that propofol would have little effect on the μOR functions in its clinically used concentrations.

The direct effects of halothane on the μOR have not been studied. In the present study, clinical concentrations of halothane (0.25 mM) had no effect on basal- and DAMGO-induced Cl^- currents in *Xenopus* oocytes expressing μOR-G_{qi5}, whereas higher concentrations of halothane (0.5 – 2.0 mM) inhibited the DAMGO-induced Cl^- currents. To our knowledge, this is the first report that shows the direct effects of halothane on the function of μOR in the heterologous expression system. Lambert et al. have reported that binding of [^{3}H]DAMGO was unaffected by lower concentrations of halothane, but 5.0% (approximately 5.3 MAC) halothane reduced its affinity (35). From our present and previous reports, higher concentrations of halothane would inhibit the DAMGO-induced currents by reducing the affinity of DAMGO to μOR. Yamakura et al., on the other hand, reported that inhibition by halothane is likely caused by inhibition of GIRK channels, not by μOR (25). Furthermore, it was recently reported that the MACs for halothane are not different between wild-type and μOR–knock-out mice (36). Although further study would be necessary, our present result suggests that halothane would have little effect on μOR in the clinical situation.

Interaction between alcohol and the CNS opioid signaling system is well established in both basic and clinical research (37, 38). However, mechanisms involving direct ethanol interaction on the μOR have not been fully elucidated. We showed that ethanol at a concentration more than 25 mM inhibited DAMGO-induced Cl^- currents in oocytes expressing μOR-G_{qi5}. Several hypotheses of such inhibitory effects have been asserted; Vukojević et al. reported that relevant concentrations of ethanol

(10 – 40 mM) altered μOR mobility and surface density and affect the dynamics of plasma membrane lipids of pheochromocytoma PC12 cells, suggesting that ethanol modified μOR activity by sorting of μOR at the plasma membrane (39). Although further studies will be required, ethanol might inhibit the DAMGO-induced currents by reducing the affinity of DAMGO to the μOR.

In conclusion, we demonstrated that ketamine and ethanol have significant inhibitory effects on the function of μOR at clinically relevant concentrations. On the other hand, halothane and propofol seem not to suppress the μOR functions at least at clinically used concentrations. Further studies will be necessary to clarify the effects of these agents on opioid systems with other assay systems. The electrophysiological method for analysis of the function of μOR fused to the chimeric Gα protein shown in this study could be useful for investigating the effects of analgesics, anesthetics, and alcohol on other $G_{i/o}$-coupled receptors.

Acknowledgments

The authors would like to thank all the members in Cancer Pathophysiology Division in National Cancer Center Research Institute. This work was supported by grants from the Ministry of Education, Culture, Sports, Science, and Technology of Japan (K.M., Y.U.); Smoking foundation (Y.U., Y.S.); Foundation of Daiichi-Sankyo Pharmaceuticals (Y.U.); a Third Term Comprehensive 10-year Strategy for Cancer Control from the Japanese Ministry of Health, Labour and Welfare; and a Grant-in-Aid for Cancer Research from the Ministry of Health, Labour and Welfare of Japan.

References

1 Harper MH, Winter PM, Johnson BH, Eger EI 2nd. Naloxone does not antagonize general anesthesia in the rat. Anesthesiology. 1978;49:3–5.
2 Pace NL, Wong KC. Failure of naloxone and naltrexone to antagonize halothane anesthesia in the dog. Anesth Analg. 1979;58:36–39.
3 Sarton E, Teppema LJ, Olievier C, Nieuwenhuijs D, Matthes HW, Kieffer BL, et al. The involvement of the mu-opioid receptor in ketamine-induced respiratory depression and antinociception. Anesth Analg. 2001;93:1495–1500.
4 Minami K, Uezono Y. G_q protein-coupled receptors as targets for anesthetics. Curr Pharm Des. 2006;12:1931–1937.
5 Durieux ME. Muscarinic signaling in the central nervous system. Recent developments and anesthetic implications. Anesthesiology. 1996;84:173–189.
6 Minami K, Gereau RW 4th, Minami M, Heinemann SF, Harris RA. Effects of ethanol and anesthetics on type 1 and 5 metabotropic glutamate receptors expressed in *Xenopus* laevis oocytes. Mol Pharmacol. 1998;53:148–156.
7 Minami K, Minami M, Harris RA. Inhibition of 5-hydroxytryptamine type 2A receptor-induced currents by n-alcohols and anesthetics. J Pharmacol Exp Ther. 1997;281:1136–1143.
8 Okamoto T, Minami K, Uezono Y, Ogata J, Shiraishi M, Shigematsu A, et al. The inhibitory effects of ketamine and pentobarbital on substance P receptors expressed in *Xenopus* oocytes. Anesth Analg. 2003;97:104–110.
9 Surratt CK, Adams WR. G protein-coupled receptor structural motifs: relevance to the opioid receptors. Curr Top Med Chem. 2005;5:315–324.
10 Minami K, Uezono Y, Ueta Y. Pharmacological aspects of the effects of tramadol on G-protein coupled receptors. J Pharmacol Sci. 2007;103:253–260.
11 Dascal N. The use of *Xenopus* oocytes for the study of ion channels. CRC Crit Rev Biochem. 1987;22:317–387.
12 Minami K, Uezono Y, Shiraishi M, Okamoto T, Ogata J, Horishita T, et al. Analysis of the effects of halothane on G_i-coupled muscarinic M_2 receptor signaling in *Xenopus* oocytes using a chimeric Gα protein. Pharmacology. 2004;72:205–212.
13 Hojo M, Sudo Y, Ando Y, Minami K, Takada M, Matsubara T, et al. μ-Opioid receptor forms a functional heterodimer with cannabinoid CB_1 receptor: electrophysiological and FRET assay analysis. J Pharmacol Sci. 2008;108:308–319.
14 Vorobiov D, Bera AK, Keren-Raifman T, Barzilai R, Dascal N. Coupling of the muscarinic M_2 receptor to G protein-activated K^+ channels via Gα_z and a receptor-Gα_z fusion protein. Fusion between the receptor and Gα_z eliminates catalytic (collision) coupling. J Biol Chem. 2000;275:4166–4170.
15 Minami K, Vanderah TW, Minami M, Harris RA. Inhibitory effects of anesthetics and ethanol on muscarinic receptors expressed in *Xenopus* oocytes. Eur J Pharmacol. 1997;339:237–244.
16 Dildy-Mayfield JE, Mihic SJ, Liu Y, Deitrich RA, Harris RA. Actions of long chain alcohols on GABAA and glutamate receptors: relation to in vivo effects. Br J Pharmacol. 1996;118:378–384.
17 Jimi N, Segawa K, Minami K, Sata T, SHigematsu A. Inhibitory effects of the intravenous anesthetic, ketamine, on rat mesangial cell proliferation. Anesth Analg. 1997;84:190–195
18 Bohm M, Schmidt U, Gieschik P, Schwinger RH, Bohm S, Erdmann E. Sensitization of adenylate cyclase by halothane in human myocardium and S49 lymphoma wild-type and cyc- cells: evidence for inactivation of the inhibitory G protein $G_i\alpha$. Mol Pharmacol. 1994;45:380–389.
19 Trimer L, Vulliemoz Y, Woo S-Y, Verosky M. Halotane effect on cAMP generation and hydrolysis in rat brain. Eur J Pharmacol. 1980;66:73–80.
20 Maas JW Jr, Vogt SK, Chan GCK, Pineda VV, Storm DR, Muglia LJ. Calcium-stimulated adenylate cyclase are critical modulators of neuronal ethanol sensitivity. J Neurosci. 2005;25:4118–4126.
21 Dascal N. Signalling via the G protein-activated K^+ channels. Cell Signal. 1997;9:551–573.
22 Uezono Y, Akihara M, Kaibara M, Kawano C, Shibuya I, Ueda Y, et al. Activation of inwardly rectifying K^+ channels by GABA-B receptors expressed in *Xenopus* oocytes. Neuroreport. 1998;9:583–587.
23 Ho BY, Uezono Y, Takada S, Takase I, Izumi F. Coupling of the expressed cannabinoid CB_1 and CB_2 receptors to phospholipase C and G protein-coupled inwardly rectifying K^+ channels. Receptors Channels. 1999;6:363–374.
24 Weigl LG, Schreibmayer W. G protein-gated inwardly rectifying potassium channels are targets for volatile anesthetics. Mol Pharmacol. 2001;60:282–289.
25 Yamakura T, Lewohl JM, Harris RA. Differential effects of general anesthetics on G protein-coupled inwardly rectifying and

other potassium channels. Anesthesiology. 2001;95:144–153.
26 Lewohl JM, Wilson WR, Mayfield RD, Brozowski SJ, Morrisett RA, Harris RA. G-protein-coupled inwardly rectifying potassium channels are targets of alcohol action. Nat Neurosci. 1999;2:1084–1090.
27 Inhibition by ketamine of muscarinic acetylcholine receptor function. Durieux ME. Anesth Analg. 1995;81:57–62.
28 Nagase Y, Kaibara M, Uezono Y, Izumi F, Sumikawa K, Taniyama K. Propofol inhibits muscarinic acetylcholine receptor-mediated signal transduction in *Xenopus* oocytes expressing the rat M_1 receptor. J Pharmacol Sci. 1999;79:319–325.
29 Kovoor A, Celver JP, Wu A, Chavkin C. Agonist induced homologous desensitization of μ-opioid receptors mediated by G protein-coupled receptor kinases is dependent on agonist efficacy. Mol Pharmacol. 1998;54:704–711.
30 Tyrosine phosphorylation of the μ-opioid receptor regulates agonist intrinsic efficacy. Mol Pharmacol. 2001;59:1360–1368.
31 Wieber J, Gugler R, Hengstmann JH, Dengler HJ. Pharmacokinetics of ketamine in man. Anaesthesist. 1975;24:260–263.
32 Idvall J, Ahlgren I, Aronsen KR, Stenberg P. Ketamine infusions: pharmacokinetics and clinical effects. Br J Anaesth. 1979;51:1167–1173.
33 Hirota K, Okawa H, Appadu BL, Grandy DK, Devi LA, Lambert DG. Stereoselective interaction of ketamine with recombinant mu, kappa, and delta opioid receptors expressed in Chinese hamster ovary cells. Anesthesiology. 1999;90:174–182.
34 Kirkpatrick T, Cockshott ID, Douglas EJ, Nimmo WS. Pharmacokinetics of propofol (diprivan) in elderly patients. Br J Anaesth. 1988;60:146–150.
35 Lambert DG, Appadu BL. Muscarinic receptor subtypes: do they have a place in clinical anaesthesia? Br J Anaesth. 1995;74:497–499.
36 Koyama T, Mayahara T, Wakamatsu T, Sora I, Fukuda K. Deletion of μ-opioid receptor in mice does not affect the minimum alveolar concentration of volatile anaesthetics and nitrous oxide-induced analgesia. Br J Anaesth. 2009;103:744–749.
37 Oswald LM, Wand GS. Opioids and alcoholism. Physiol Behav. 2004;81:339–358.
38 Herz A. Endogenous opioid systems and alcohol addiction. Psychopharmacology (Berl). 1997;129:99–111.
39 Vukojevic V, Ming Y, D'Addario C, Rigler R, Johansson B, Terenius L. Ethanol/naltrexone interactions at the mu-opioid receptor. CLSM/FCS study in live cells. PLoS One. 2008;3:e4008.

Neuropharmacology 57 (2009) 311–321

Contents lists available at ScienceDirect

Neuropharmacology

journal homepage: www.elsevier.com/locate/neuropharm

Chronic lithium treatment up-regulates cell surface $Na_V1.7$ sodium channels via inhibition of glycogen synthase kinase-3 in adrenal chromaffin cells: Enhancement of Na^+ influx, Ca^{2+} influx and catecholamine secretion after lithium withdrawal

Toshihiko Yanagita [a,*], Toyoaki Maruta [a], Takayuki Nemoto [a], Yasuhito Uezono [b,c], Kiyotaka Matsuo [b], Shinya Satoh [a], Norie Yoshikawa [a], Tasuku Kanai [a], Hideyuki Kobayashi [a], Akihiko Wada [a]

[a] Department of Pharmacology, Miyazaki Medical College, University of Miyazaki, Kiyotake, Miyazaki 889-1692, Japan
[b] Department of Pharmacology, Nagasaki University, Graduate School of Biomedical Sciences, Nagasaki 852-8523, Japan
[c] Cancer Pathophysiology Division, National Cancer Center Research Institute, Tokyo 104-0045, Japan

ARTICLE INFO

Article history:
Received 29 September 2008
Received in revised form
1 May 2009
Accepted 20 May 2009

Keywords:
Lithium
Sodium channel
Up-regulation
Glycogen synthase kinase-3
Transcription
Adrenal chromaffin cells

ABSTRACT

In cultured bovine adrenal chromaffin cells expressing $Na_V1.7$ isoform of voltage-dependent Na^+ channels, we have previously reported that lithium chloride (LiCl) inhibits function of Na^+ channels independent of glycogen synthase kinase-3 (GSK-3) (Yanagita et al., 2007). Here, we further examined the effects of chronic lithium treatment on Na^+ channels. LiCl treatment (1–30 mM, ≥12 h) increased cell surface [^{3}H]saxitoxin ([^{3}H]STX) binding by ~32% without altering the affinity of [^{3}H]STX binding. This increase was prevented by cycloheximide and actinomycin D. SB216763 and SB415286 (GSK-3 inhibitors) also increased cell surface [^{3}H]STX binding by ~31%. Simultaneous treatment with LiCl and SB216763 or SB415286 did not produce an increased effect on [^{3}H]STX binding compared with either treatment alone. LiCl increased Na^+ channel α-subunit mRNA level by 32% at 24 h. LiCl accelerated α-subunit gene transcription by 35% without altering α-subunit mRNA stability. In LiCl-treated cells, LiCl inhibited veratridine-induced $^{22}Na^+$ influx as in untreated cells. However, washout of LiCl after chronic treatment enhanced veratridine-induced $^{22}Na^+$ influx, $^{45}Ca^{2+}$ influx and catecholamine secretion by ~30%. Washout of LiCl after 24 h treatment shifted concentration–response curve of veratridine upon $^{22}Na^+$ influx upward, without altering its EC_{50} value. *Ptychodiscus brevis* toxin-3 allosterically enhanced veratridine-induced $^{22}Na^+$ influx by two-fold in untreated and LiCl-treated cells. Whole-cell patch-clamp analysis indicated that *I–V* curve and steady-state inactivation/activation curves were comparable between untreated and LiCl-treated cells. Thus, GSK-3 inhibition by LiCl up-regulated cell surface $Na_V1.7$ via acceleration of α-subunit gene transcription, enhancing veratridine-induced Na^+ influx, Ca^{2+} influx and catecholamine secretion.

1. Introduction

Density and activity of cell surface voltage-dependent Na^+ channels are fluctuated to accommodate development, differentiation, and survival of excitable cells (Linsdell and Moody, 1994; Yanagita et al., 2003), whereas the regulatory mechanisms of Na^+ channels remain largely unknown. Aberrant expression and activity of Na^+ channels are associated with hypoxia/ischemia-induced cell injury, seizures, fatal cardiac arrhythmias, and intolerable pain (Catterall, 2000; Wada, 2006; Waxman et al., 2000). To understand the molecular basis for these physiological and pathological events, it is essential to explore the mechanisms by which the expression and function of cell surface Na^+ channels are regulated.

Na^+ channels consist of the principal α-subunit (~260 kDa), without or with auxiliary β_1 ~ β_4-subunit (~38 kDa), depending on the tissues and species (Catterall, 2000; Wada, 2006). The α-subunit forms the ion-pore and the toxin binding sites [e.g., site 1 for tetrodotoxin (TTX)/saxitoxin (STX), site 2 for veratridine, and site 5 for *Ptychodiscus brevis* toxin-3 (PbTx-3)] (Catterall, 2000). The nine isoforms of α-subunits ($Na_V1.1$–$Na_V1.9$) arise from nine different genes (SCN1A-SCN5A and SCN8A-SCN11A) (Wada, 2006).

Lithium is the most commonly used drug for the treatment of bipolar disorder (BPD), but the therapeutic mechanism of action remains unclear (Gurvich and Klein, 2002). Recent studies indicate

* Corresponding author. Tel.: +81 985 85 1786; fax: +81 985 84 2776.
E-mail address: yanagita@med.miyazaki-u.ac.jp (T. Yanagita).

0028-3908/$ – see front matter © 2009 Elsevier Ltd. All rights reserved.
doi:10.1016/j.neuropharm.2009.05.006

that lithium has neurotrophic and neuroprotective effects against various noxious insults (e.g., ischemia, glutamate excitotoxicity, β-amyloid), and protects against neurodegenerative diseases in both human patients and animal models (e.g., Alzheimer's diseases, Parkinson's disease, Huntington's disease) (Gurvich and Klein, 2002; Wada et al., 2005).

Glycogen synthase kinase-3 (GSK-3), a serine/threonine protein kinase, is one of the key targets of the neurotrophic/neuroprotective effects of lithium (Gurvich and Klein, 2002; Jope, 2003; Wada et al., 2005). GSK-3 consists of α and β isoforms, and its activity is inhibited by therapeutic concentrations of lithium (Ryves and Harwood, 2001). We have recently reported that acute exposure to lithium inhibited the function of Na^+ channels independent of GSK-3 inhibition (Yanagita et al., 2007). However, it is unknown whether chronic lithium treatment could modulate the density and function of Na^+ channels in all tissues.

In adrenal chromaffin cells (embryologically derived from neural crest), α-subunit isoform of Na^+ channels is $Na_V1.7$ (the TTX/STX-sensitive human neuroendocrine-type Na^+ channel α-subunit [hNE-Na]) (Klugbauer et al., 1995). In cultured bovine adrenal chromaffin cells, we have demonstrated that cell surface Na^+ channels are up- and down-regulated by extra- and intra-cellular signaling. For example, protein kinase C-ε and extracellular signal-regulated kinase destabilized $Na_V1.7$ mRNA, and protein kinase C-α promoted internalization of Na^+ channels (Yanagita et al., 2000, 2003). Several bioactive signaling molecules and therapeutic drugs that would be considered neuroprotective (e.g., lysophosphatidic acid [Maruta et al., 2008], valproic acid [Yamamoto et al., 1997], insulin, carvedilol, cyclosporine A, FK506 and NS-7) up-regulated Na^+ channels via multiple mechanisms (reviewed in Wada et al., 2004). In the present study, we found that chronic lithium treatment up-regulated cell surface Na^+ channels via inhibition of GSK-3, resulting in the enhancement of Na^+ influx, Ca^{2+} channel gating and catecholamine secretion.

2. Materials and methods

2.1. Materials

Eagle's minimum essential medium was purchased from Nissui Seiyaku (Tokyo, Japan). Calf serum and TRIzol reagent were from Invitrogen Corp. (Carlsbad, CA, USA). Actinomycin D, cycloheximide, cytosine arabinoside, lithium chloride (LiCl), tetrodotoxin (TTX), ouabain and veratridine were from Sigma (St. Louis, MO, USA). *Ptychodiscus brevis* toxin-3 (PbTx-3) was from Latoxan, Westbury, (NY, USA). SB216763 and SB425286 were from Tocris Cookson Ltd. (Avonmouth, UK). Oligotex-dT30<Super> and mini Quick Spin RNA Columns were from Roche Diagnostics (Tokyo, Japan). The BcaBEST labeling kit was from Takara (Shiga, Japan). RQ1 RNase-Free DNase and proteinase K were from Promega (Madison, WI, USA). [^{3}H]STX (20–40 Ci/mmol), [α-^{32}P]dCTP (>3000 Ci/mmol), [α-^{32}P]UTP (800 Ci/mmol), [γ-^{32}P]ATP (~3000 Ci/mmol), Hybond-N^+, and Rapid-hyb buffer were from GE Healthcare Biosciences (Piscataway, NJ). cDNA for human glyceraldehyde 3-phosphate dehydrogenase (GAPDH) was from Clontech (Palo Alto, CA, USA). Plasmid Bluescript II (pBII) was from Stratagene (La Jolla, CA, USA). Plasmids containing hNE-Na cDNA (Klugbauer et al., 1995) and rat brain Na^+ channel β_1-subunit cDNA (Oh and Waxman, 1994) were generously donated by Drs. F. Hofmann (Technischen Universität München), and Y. Oh (University of Alabama), respectively.

2.2. Primary culture of adrenal chromaffin cells and drug treatment

Isolated bovine adrenal chromaffin cells were cultured (4×10^6/dish, Falcon; 35 mm in diameter) under 5% CO_2/95% air in a CO_2 incubator in Eagle's minimum essential medium containing 10% calf serum, and 3 μM cytosine arabinoside to suppress the proliferation of nonchromaffin cells (Yamamoto et al., 1997; Yanagita et al., 2000). Three days after plating, the cells were exposed to test compounds for up to 72 h. Test compounds were dissolved in distilled H_2O or dimethyl sulfoxide (DMSO), and the final concentration of DMSO in the test medium was 0.25%. Treatment of chromaffin cells with 0.25% DMSO for 72 h did not alter [^{3}H]STX binding, in contrast to untreated cells. When chromaffin cells were purified by differential plating (Yamamoto et al., 1997; Yanagita et al., 2000), the relative abundance of α- and β_1-subunit mRNAs/GAPDH mRNA was similar for conventional and purified adrenal chromaffin cells.

2.3. [^{3}H]STX binding

Cells were washed with ice-cold Krebs–Ringer phosphate (KRP) buffer (mM) (154 NaCl, 5.6 KCl, 1.1 $MgSO_4$, 2.2 $CaCl_2$, 0.85 NaH_2PO_4, 2.15 Na_2HPO_4, 5 glucose, and 0.5% bovine serum albumin, pH 7.4) and incubated with 1–25 nM [^{3}H]STX in 1 ml KRP buffer at 4 °C for 15 min in the absence (total binding) and presence (nonspecific binding) of 1 μM TTX (Yamamoto et al., 1997; Yanagita et al., 2000). The cells were washed, solubilized in 10% Triton X-100 and counted for radioactivity. Specific binding was calculated as the total binding minus nonspecific binding.

2.4. $^{22}Na^+$ influx, $^{45}Ca^{2+}$ influx, and catecholamine secretion

$^{22}Na^+$ influx was measured by incubating cells with 2 μCi $^{22}NaCl$ in culture medium or KRP buffer at 37 °C for 5 min with or without veratridine, PbTx-3 and ouabain, and for 1 min with or without nicotine or high K^+ solution. To measure $^{45}Ca^{2+}$ influx and catecholamine secretion, cells were incubated with 2 μCi $^{45}CaCl_2$ for 5 min with or without veratridine in KRP buffer, or for 1 min with or without nicotine or high K^+ solution. Incubation medium was saved in a test tube for catecholamine assay by HPLC, and the cells were washed, solubilized and counted for radioactivity (Yamamoto et al., 1997).

2.5. Electrophysiological recordings

The whole-cell patch-clamp technique was used to study macroscopic Na^+ currents at room temperature (22.5–23.5 °C) in untreated and LiCl (20 mM for 24 h)-treated cells. Command voltages were programmed by pCLAMP software (Axon Instruments, Foster City, CA) and delivered by a List EPC7 voltage clamp amplifier (List-Electronic, Darmstadt, Germany). The data were filtered at 5 kHz. Pipette resistance was 1.5–2.5 MΩ. Most of the capacitative current was canceled by the EPC7 circuitry. Any remaining capacitative artifact and leakage current were subtracted by the P/-4 method (Hamill et al., 1981). Voltage errors were minimized using series resistance compensation (generally 80%). The data were analyzed using ClampFit (Axon Instruments, Union City, CA) and SigmaPlot (SPSS Inc., Chicago, IL). The bath solution contained 145 mM NaCl, 4 mM KCl, 1.8 mM $CaCl_2$, 1.0 mM $MgCl_2$, 10 mM HEPES, adjusted to pH 7.35 with NaOH, and the pipette solution contained 10 mM NaF, 110 mM CsF, 20 mM CsCl, 10 mM EGTA and 10 mM HEPES, pH 7.35 with CsOH (Maruta et al., 2008).

For the current–voltage curve, the peak Na^+ current (I) was elicited by 20 ms pulses in 10 mV incremental steps from −90 mV to 90 mV, with holding potential of −120 mV. I was normalized to the maximum I (I_{max}) and plotted. The steady-state activation curve was obtained by calculating the equation: $G = I/(V - V_{rev})$ (G, the conductance; V, each membrane potential; V_{rev}, the reversal potential).

For the steady-state inactivation curve, I was measured with a 20 ms test pulse to −20 mV after a series of 100 ms prepulses from −150 mV to −30 mV at 10 mV incremental steps, with holding potential of −120 mV.

The steady-state activation and inactivation curves were fitted with the Boltzmann equation: $G/G_{max} = (1 + \exp[(V - V_{1/2})/k])^{-1}$ and $I/I_{max} = (1 + \exp[(V - V_{1/2})/k])^{-1}$ ($V_{1/2}$, membrane potential for midpoint of activation/inactivation; k, slope factor).

2.6. Northern blot

The total cellular RNA was isolated from the cells by acid guanidine thiocyanate phenol–chloroform extraction using a TRIzol reagent. Poly $(A)^+$ RNA was purified by Oligotex-dT30<Super>, electrophoresed on a 1% agarose gel containing 6.3% formaldehyde in the buffer (40 mM 3-(N-morpholino) propanesulfonic acid, pH 7.2, 0.5 mM EDTA and 5 mM sodium citrate), transferred to a nylon membrane (Hybond-N^+, Amersham) in 20× saline-sodium citrate (SSC; 1× SSC = 0.15 M NaCl and 0.015 M sodium citrate) overnight and cross-linked using a UV cross-linker (Funakoshi, Tokyo, Japan).

Plasmids containing hNE-Na cDNA and β_1-subunit cDNA were digested with MunI and SacII plus HindIII, respectively, to obtain nucleotide (nt) fragments including the α-subunit (nt 1365–2948) and β_1-subunit (nt 457–790) (Yanagita et al., 2003). These cDNA fragments and GAPDH cDNA (1.1 kbp) were labeled with [α-^{32}P]dCTP using a BcaBEST labeling kit. The membrane was prehybridized then hybridized with the hNE-Na probe at 65 °C for 4 h in Rapid-hyb buffer. The membrane was washed twice in 0.2× SSC containing 0.1% SDS for 30 min and subjected to autoradiography. The same membrane was successively hybridized with probes for the β_1-subunit, then GAPDH after being washed with 0.1% SDS at 100 °C to remove the former probe. Autoradiograms were quantified by a bioimage analyzer BAS 2000.

2.7. Nuclear run-on assay

Cells were washed twice with ice-cold PBS, dislodged and centrifuged at 500 × g for 5 min. Cell pellets were suspended in buffer A (10 mM Tris–HCl, pH 7.4, 10 mM NaCl, 3 mM $MgCl_2$, and 0.4% Nonidet P-40), treated on ice for 5 min, and centrifuged at 500 × g for 5 min. Nuclear pellets were washed with buffer A and suspended in buffer B (50 mM Tris–HCl, pH 8.3, 40% glycerol, 5 mM $MgCl_2$, and 0.1 mM EDTA).

Nuclei (1.2×10^7/100 μl) were incubated at 30 °C for 30 min with 100 μl buffer C (10 mM Tris–HCl, pH 8.0, 5 mM $MgCl_2$, 200 mM KCl, 2 mM dithiothreitol, 0.5 mM of each of ATP, CTP, GTP, and 200 μCi [α-^{32}P]UTP); then the DNA was digested by exposure to 2U RQ1 RNase-Free DNase for 10 min at 30 °C. Proteins were digested in 200 μl buffer D (20 mM Tris–HCl, pH 7.4, 10 mM EDTA, 20% SDS, and 200 μg/ml proteinase K) at 50 °C for 1 h. Newly-transcribed RNAs were extracted using TRIzol reagent, dissolved in TE (10 mM Tris–HCl, pH 7.5 and 1 mM EDTA), and purified using mini Quick Spin RNA Columns. ^{32}P-Labeled RNAs (5×10^6 cpm/ml) were hybridized overnight at 70 °C in Rapid-hyb buffer, with a nylon membrane immobilizing 10 μg pBII alone, and pBII containing hNE-Na cDNA or GAPDH cDNA. The hNE-Na cDNA fragment (nt 1–2253) was liberated by digesting the hNE-Na plasmid (Klugbauer et al., 1995) with KpnI and BglII, and subcloned into pBII (Yanagita et al., 2003). The membrane was sequentially washed in 2× SSC containing 0.1% SDS at 65 °C for 15 min, in 2× SSC containing 10 μg/ml RNase A at 37 °C for 10 min, and in 0.2× SSC containing 0.1% SDS at 65 °C for 10 min. The membrane was then subjected to autoradiography.

2.8. Statistical methods

[^{3}H]STX binding, $^{22}Na^+$ influx, $^{45}Ca^{2+}$ influx and catecholamine secretion were measured in triplicate, and all experiments were repeated at least three times to obtain means and standard errors. Significance ($P < 0.05$) was determined by one-way analysis of variance with post-hoc mean comparison by the Newman–Keuls multiple range test.

3. Results

3.1. Concentration- and time-dependent increase of cell surface [^{3}H]STX binding by chronic treatment with LiCl: prevention by cycloheximide and actinomycin D

To evaluate the effect of chronic LiCl treatment on the cell surface density of Na^+ channels, adrenal chromaffin cells were treated with or without 1–30 mM LiCl for 24 h, and [^{3}H]STX binding was assayed (Fig. 1a). LiCl increased cell surface [^{3}H]STX binding in a concentration-dependent manner, with an EC_{50} value of 1.2 mM. A significant increase in [^{3}H]STX binding in response to LiCl was observed with a dose of 1 mM, and the maximal increase was observed with a dose of 20 mM. In contrast, 20 mM sodium chloride (NaCl) had little effect on [^{3}H]STX binding (Fig. 1a). The increase in binding became evident within 12 h of treatment with 20 mM LiCl, reaching the near maximal increase of 32% at 24 h (Fig. 1b). The effect of LiCl was reversible because washing the cells with culture medium followed by an additional 24 h incubation without LiCl restored [^{3}H]STX binding to 108% of the binding values of untreated cells (data not shown). Scatchard plot analysis (Fig. 1c) revealed that LiCl treatment (20 mM, 24 h) significantly raised the B_{max} values from 56.8 ± 5.6 to 74.9 ± 5.7 fmol/4×10^6 cells without altering the K_d values (4.4 ± 0.5 nM, untreated cells; 4.7 ± 0.6 nM, LiCl-treated cells; $n = 3$). Because LiCl-induced up-regulation of [^{3}H]STX binding required chronic (≥12 h) LiCl treatment, we examined whether LiCl-induced up-regulation of [^{3}H]STX binding could require *de novo* synthesis of protein(s). As shown in Fig. 1d, both cycloheximide (10 μg/ml), an inhibitor of protein synthesis, and actinomycin D (10 μg/ml), an inhibitor of RNA synthesis, slightly decreased [^{3}H]STX binding but completely prevented the increased [^{3}H]STX binding caused by LiCl treatment.

3.2. Concentration- and time-dependent increase of cell surface [^{3}H]STX binding by SB216763 and SB415286: the lack of an additional increasing effect for LiCl

Evidence has accumulated that LiCl inhibits GSK-3 activity, and this inhibition is crucial for the therapeutic action of lithium (Gurvich and Klein, 2002; Jope, 2003). To test whether GSK-3 could be involved in the increased binding effect of lithium, we examined the effects of GSK-3 inhibitors (SB216763 and SB415286) on the LiCl-induced increase of [^{3}H]STX binding (Fig. 2a).

As shown in Fig. 2a, SB216763 (10 μM) and SB415286 (10 μM) each increased [^{3}H]STX binding by ~31%. Simultaneous treatment with LiCl and SB216763 or SB415286 did not have a greater effect on [^{3}H]STX binding than either treatment alone. Because SB216763 (10 μM) and SB415286 (10 μM) increased [^{3}H]STX binding and did not further increase binding with concurrent LiCl treatment, we further examined the effects of SB216763 and SB415286 on [^{3}H]STX binding. Cells were treated with or without 1–30 μM SB216763 or SB415286 for 24 h, and the [^{3}H]STX binding was assayed (Fig. 2b). Treatment with SB216763 or SB415286 for 24 h increased cell surface [^{3}H]STX binding by 31% and 25%, respectively, in a concentration-dependent manner, with EC_{50} values of 2.6 and 2.8 μM, respectively. The EC_{50} values of SB216763 and SB415286 for the increased [^{3}H]STX binding were comparable with the EC_{50} values of SB216763 (3.6 μM) and SB415286 (2.9 μM) for stimulation of glycogen synthesis in Chinese hamster ovary cells (Coghlan et al., 2000).

The increase in the binding became evident within 12 h of treatment with SB216763 (10 μM) or SB415286 (10 μM), reaching the almost maximal increase of 33% and 29%, respectively, at 48 h (Fig. 2c). The effects of both SB216763 and SB415286 were reversible because washing the cells with culture medium followed by an additional 24 h incubation without these compounds restored [^{3}H]STX binding to ~105% of the binding seen in untreated cells (data not shown). Scatchard plot analysis (Fig. 2d) showed that SB216763 (10 μM for 24 h) or SB415286 (10 μM for 24 h) increased the B_{max} values from 57.5 ± 5.8 to 75.2 ± 4.8 or 71.5 ± 4.1 fmol/4×10^6 cells, respectively, without altering K_d values (4.1 ± 0.5 nM, untreated cells; 4.4 ± 0.4 nM, SB216763-treated cells; 4.2 ± 0.4 nM, SB415286-treated cells; $n = 3$).

3.3. Up-regulation of Na^+ channel α- (but not β_1-) subunit mRNA level in cells treated with LiCl

Because up-regulation of [^{3}H]STX binding by LiCl was dependent on translation, we examined whether LiCl treatment may increases Na^+ channel α- and β_1-subunit mRNA levels. Cells were treated with or without 20 mM LiCl for up to 24 h, and the steady-state levels of Na^+ channel α- and β_1-subunit mRNAs were measured by northern blot analysis (Fig. 3a). In our present study, the hNE-Na probe hybridized to one major (~9.4 kb) and two minor (~11.0 and ~7.0 kb) transcripts, while the β_1-subunit probe hybridized to a single (~1.5 kb) transcript, as reported previously (Yanagita et al., 2000; Maruta et al., 2008). Levels of α (9.4 kb)- and β_1-subunit mRNAs were normalized to GAPDH mRNA levels (Fig. 3b and c). LiCl raised the α- (but not β_1-) subunit mRNA level by ~12% as early as 3 h and reached a plateau at a maximal increase of ~32% between 24 and 48 h ($t_{1/2} = 8.2$ h).

3.4. Acceleration of transcription rate of Na^+ channel α-subunit gene by LiCl: no effect on α-subunit mRNA stability

Because LiCl raised the steady-state level of Na^+ channel α-subunit mRNA, we examined whether LiCl treatment may affect transcription of the α-subunit gene and/or stability of α-subunit mRNA. Cells were treated with or without 20 mM LiCl for 12 h, and the transcription rate of the α-subunit gene was measured by nuclear run-on assay (Yanagita et al., 2003). LiCl accelerated transcription of the α-subunit gene by 30% (Fig. 4a).

We then measured the degradation rate of α-subunit mRNA by using actinomycin D. As shown in Fig. 4b, cells were treated for the first 12 h with or without 20 mM LiCl, then exposed to actinomycin D in the continuous presence or absence of either test treatment and subjected to northern blot analysis at the indicated times. LiCl did not alter the half-life ($t_{1/2}$) of α-subunit mRNA (~9.4 kb).

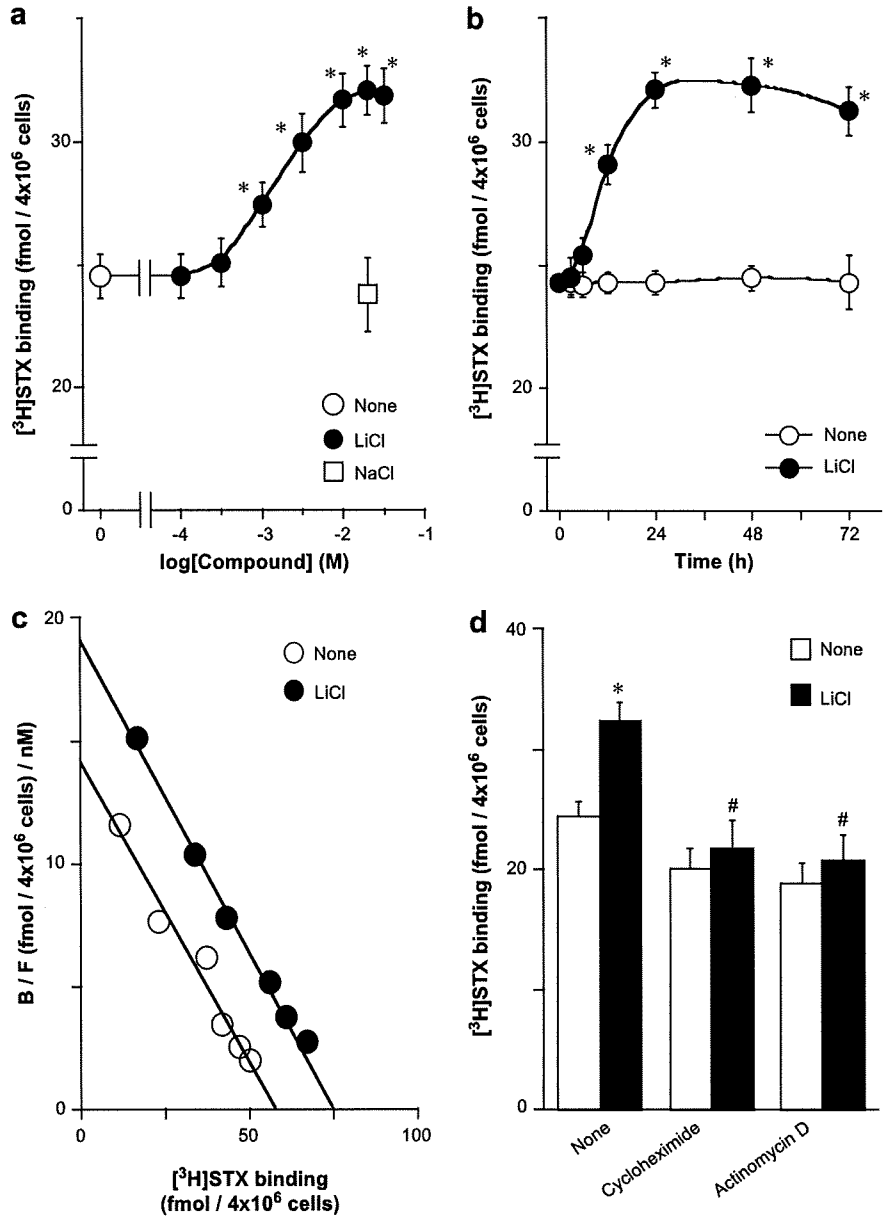

Fig. 1. Concentration- and time-dependent increase in cell surface [^{3}H]STX binding by LiCl, but not by NaCl: prevention by cycloheximide and actinomycin D. (a) Cells were treated with or without indicated concentrations of LiCl or NaCl for 24 h, and subjected to [^{3}H]STX binding. Mean ± S.E.M. ($n = 5$). *$P < 0.05$, compared with untreated cells. (b) Cells were treated with or without 20 mM LiCl for up to 72 h, and subjected to [^{3}H]STX binding assay at the indicated times. Mean ± S.E.M. ($n = 5$). *$P < 0.05$, compared with untreated cells. (c) Scatchard plot analysis of [^{3}H]STX binding in cells treated with or without 20 mM LiCl for 24 h. Data are representative of three independent experiments with similar results. (d) Cells were treated with (closed columns) or without (open columns) 20 mM LiCl for 24 h in the presence or absence of 10 μg/ml cycloheximide or 10 μg/ml Actinomycin D and subjected to [^{3}H]STX binding assay. Mean ± S.E.M. ($n = 3$). *$P < 0.05$, compared with cells not treated with LiCl; #, no significant difference within each cell group.

3.5. Up-regulation of veratridine-induced $^{22}Na^+$ influx in cells chronically treated with LiCl and SB216763: inhibition by acute treatment with LiCl and increase by LiCl removal after chronic treatment

In adrenal chromaffin cells, our previous study demonstrated that acute (5 min) treatment with LiCl inhibited veratridine-induced $^{22}Na^+$ influx in a concentration-dependent manner independent of GSK-3 inhibition, without altering pharmacological properties of Na^+ channels; LiCl (20 mM) inhibited veratridine-induced $^{22}Na^+$ influx by 41%, whereas SB216763 and SB415286 did not affect veratridine-induced $^{22}Na^+$ influx (Yanagita et al., 2007). In the present study, we further examined whether chronic treatment with LiCl or SB216763 affects Na^+ influx. Cells were treated with or without 20 mM LiCl or 10 μM SB216763 for up to 48 h. At the end of treatment periods, cells were exposed to 2 μCi $^{22}NaCl$ with or without 100 μM veratridine for an additional 5 min in the continuous presence or absence of 20 mM LiCl or 10 μM SB216763. As shown in Fig. 5a, chronic LiCl treatment inhibited veratridine-induced $^{22}Na^+$ influx regardless of treatment time with LiCl (1, 12, 24 or 48 h). In contrast, chronic (>12 h) SB216763 treatment increased veratridine-induced $^{22}Na^+$ influx in a time-dependent manner by ~30%. SB415286 treatment also increased veratridine-induced $^{22}Na^+$ influx by 28% (data not shown).

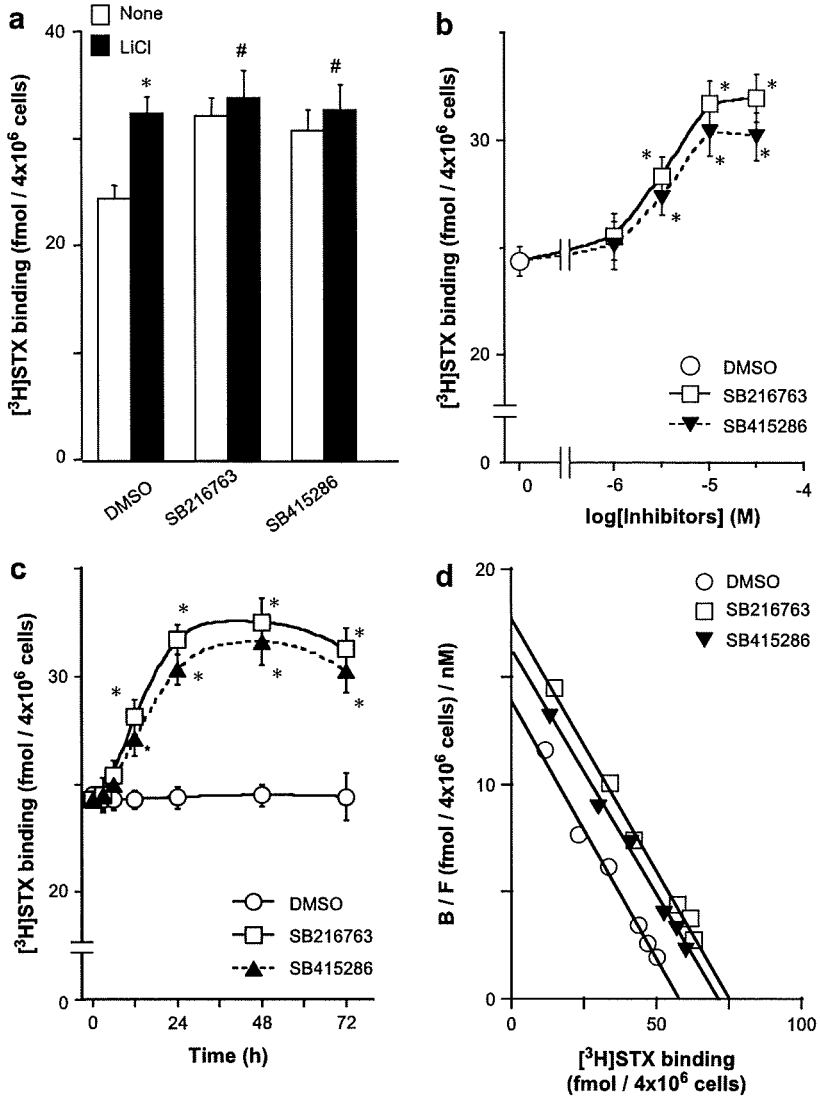

Fig. 2. Concentration- and time-dependent increase in cell surface [^{3}H]STX binding by SB216763 and SB415286: no additional increasing effect between SB216763, SB415286 and LiCl. (a) Cells were treated with (closed columns) or without (open columns) 20 mM LiCl for 24 h in the presence or absence of 10 μM SB216763 or 10 μM SB415286, and subjected to [^{3}H]STX binding assay. Mean ± S.E.M. ($n = 3$). *$P < 0.05$, compared with cells not treated with LiCl; #, no significant difference within each cell group. (b) Cells were treated with or without indicated concentrations of SB216763 or SB415286 for 24 h and subjected to [^{3}H]STX binding. Mean ± S.E.M. ($n = 5$). *$P < 0.05$, compared with untreated cells. (c) Cells were treated with or without 10 μM SB216763 or 10 μM for up to 72 h and subjected to [^{3}H]STX binding assay at the indicated times. Mean ± S.E.M. ($n = 5$). *$P < 0.05$, compared with untreated cells; #$P < 0.05$, compared with test drug-treated cells. (d) Scatchard plot analysis of [^{3}H]STX binding in cells treated with or without 10 μM SB216763 or 10 μM SB415286 for 24 h. Data are representative of three independent experiments with similar results.

We also examined how Na^+ channels respond to removal of LiCl or SB216763 after chronic treatment. Cells were treated with or without 20 mM LiCl (Fig. 5b) or 10 μM SB216763 (Fig. 5c) for up to 48 h, and washed with KRP buffer to remove LiCl or SB216763. Cells were then incubated with or without 100 μM veratridine for 5 min in KRP buffer containing 2 μCi $^{22}NaCl$ in the presence or absence of 20 mM LiCl (Fig. 5b) or 10 μM SB216763 (Fig. 5c). As shown in Fig. 5b, washout of LiCl after chronic treatment increased veratridine-induced $^{22}Na^+$ influx in a time-dependent manner by ~33%. However, re-exposure to LiCl also inhibited veratridine-induced $^{22}Na^+$ influx, as in LiCl-untreated cells (0 h). Whereas, in SB216763-treated cells (Fig. 5c), the increase of veratridine-induced $^{22}Na^+$ influx caused by chronic (>12 h) treatment with SB216763 was also observed, regardless of SB216763 washout or re-exposure to SB216763. Similar results were obtained from SB415286-treated cells (data not shown).

3.6. *Pharmacological properties of Na^+ channels: similarity between untreated, LiCl-treated and SB216763-treated cells*

Because removal of LiCl after chronic treatment and chronic treatment with SB216763 increased veratridine-induced $^{22}Na^+$ influx, we evaluated the pharmacological properties of Na^+ channels by using neurotoxins. Cells were treated with or without 20 mM LiCl or 10 μM SB216763 for 24 h and washed with KRP buffer; then $^{22}Na^+$ influx was assayed. In adrenal chromaffin cells, veratridine, a toxin acting at site 2 in segment 6 of domain I (DIS6) of the Na^+ channel α-subunit (Cestèle and Catterall, 2000), causes a persistent influx of $^{22}Na^+$, for at least 5 min, that passes through TTX/STX-sensitive Na^+ channels (Yamamoto et al., 1997). Fig. 6a shows that in cells treated with LiCl or SB216763, veratridine-induced $^{22}Na^+$ influx was augmented by ~35% with no change in

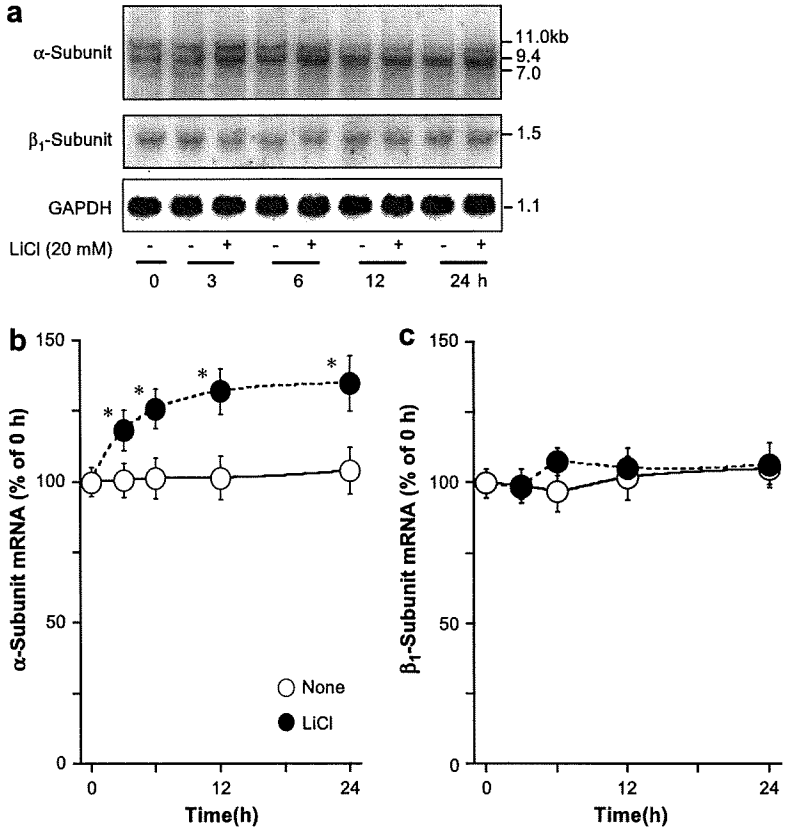

Fig. 3. Northern blot analysis: up-regulation of $Na_V1.7$ Na^+ channel α- (but not β_1-) subunit mRNA level in cells treated with LiCl. (a) Cells were treated with (+) or without (−) 20 mM LiCl for up to 24 h; then poly $(A)^+$ RNA was extracted, electrophoresed, and transferred to membrane. The membrane was hybridized with each ^{32}P-labeled cDNA probe for hNE-Na (top), Na^+ channel β_1-subunit (middle), or GAPDH (bottom) after removing the former probe. Levels of α-subunit mRNA (~9.4 kb), β_1-subunit mRNA and GAPDH mRNA were quantified by a bioimage analyzer. The relative level of (b) α- or (c) β_1-subunit mRNA/GAPDH mRNA is shown. The relative level in untreated cells at 0 h is assigned a value of 100%. Mean ± S.E.M. ($n = 3$). *$P < 0.05$, compared with untreated cells.

EC_{50} values of veratridine (84 μM, untreated cells; 87 μM, LiCl-treated cells; 86 μM, SB216763-treated cells).

Fig. 6b shows that veratridine-induced $^{22}Na^+$ influx was abolished by treatment with 1 μM TTX, consistent with TTX/STX-sensitive $Na_V1.7$ channels (Klugbauer et al., 1995). We then characterized pharmacological properties of Na^+ channels using PbTx-3, a toxin acting at site 5 between DIVS5 and DIS6 of the Na^+ channel α-subunit (Cestèle and Catterall, 2000). Fig. 6b shows that PbTx-3 (1 μM) alone had little effect, but it enhanced veratridine (100 μM)-induced $^{22}Na^+$ influx by approximately 2-fold in cells treated with LiCl or SB216763, which were similar to its effects on untreated cells.

Our previous study showed that Na^+ influx increases the activity of Na^+, K^+-ATPase, whereby Na^+, once entering chromaffin cells, is continuously pumped out (Yamamoto et al., 1997). As shown in Fig. 6b, ouabain at 100 μM, a concentration that completely inhibits the activity of Na^+, K^+-ATPase (Yamamoto et al., 1997), increased the accumulation of $^{22}Na^+$, and this was not changed by treatment with LiCl. In the presence of ouabain, veratridine (100 μM)-induced $^{22}Na^+$ influx occurred to a greater extent in cells treated with LiCl or SB216763, compared with untreated cells.

3.7. Electrophysiological properties of Na^+ currents: similarity between untreated and LiCl-treated cells

We also examined electrophysiological properties of Na^+ channels using the whole-cell patch-clamp technique on single adrenal chromaffin cells (Maruta et al., 2008). Cells were treated with or without 20 mM LiCl for 24 h and in the presence or absence of 1 μM tetrodotoxin (TTX). As shown in Fig. 7a, TTX sensitive Na^+ currents were recorded in both control and pretreated cells. Fig. 7b shows the *I–V* relationship for Na^+ current recorded in adrenal chromaffin cells. The results indicate that in cells pretreated with LiCl, Na^+ current activation was more sensitive to voltage shifts, as shown by a slightly steeper *I–V* curve with a peak that is ~10 mV more negative compared to the control. Fig. 7c shows the voltage-dependence of steady-state inactivation and activation measured in control cells and cells treated with LiCl. The steady-state inactivation curve shows that the voltage step that elicited 50% of the maximal current was shifted to 6 mV more hyperpolarizing in cells pretreated with LiCl, although this shift was not significant (-71.8 ± 2.6 mV; $n = 8$ vs. -65.9 ± 1.9 mV; $n = 12$). Analysis of the steady-state activation curve showed that there was no significant difference in the voltage step that elicited 50% of the maximal current amplitude between control (-32.8 ± 2.8 mV, $n = 12$) and LiCl-treated cells (-37.8 ± 1.2 mV, $n = 8$).

3.8. Effects of LiCl treatment on $^{45}Ca^{2+}$ influx via voltage-dependent Ca^{2+} channels and catecholamine secretion

In adrenal chromaffin cells, our previous studies showed that veratridine-induced Na^+ influx via Na^+ channels is necessary for the gating of voltage-dependent Ca^{2+} channels, which is a prerequisite for exocytic secretion of catecholamines (Yamamoto et al., 1997). However, a high K^+ concentration directly gates voltage-dependent

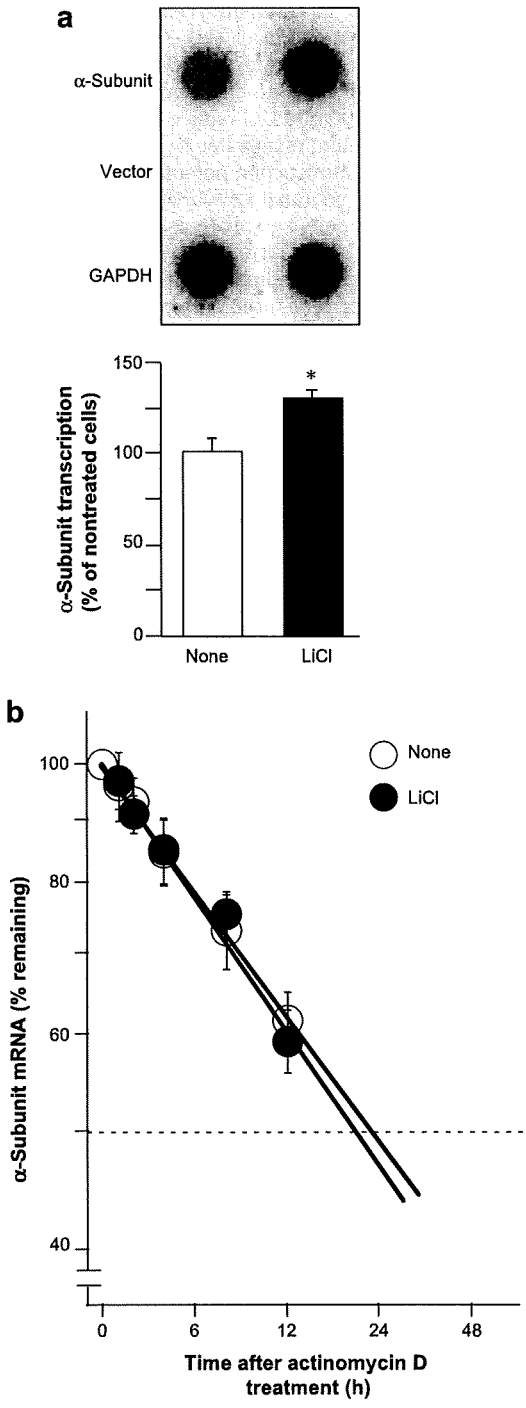

Fig. 4. Increased transcription rate of $Na_V1.7$ Na^+ channel α-subunit gene in cells treated with LiCl: no effect on α-subunit mRNA stability. (a) Cells were treated with or without 20 mM LiCl for 12 h; then nuclei were isolated and used for in vitro nuclear run-on assay using [α-^{32}P]UTP. ^{32}P-labeled transcripts were purified, and hybridized to 10 μg of pBII alone (Vector) or pBII containing hNE-Na cDNA (α-subunit) or GAPDH cDNA immobilized on membrane (upper panel). Data are typical of three independent experiments with similar results. Radioactivities in the upper panel were quantified by a bioimage analyzer, and transcription rates of α-subunit gene are shown in lower panel; a value of 100% represents the transcription rate obtained in cells not subjected to a 12 h incubation. (b) Cells were pretreated with or without 20 mM LiCl for 12 h and incubated with 10 μg/ml actinomycin D in the continuous presence or absence of 20 mM LiCl. At the indicated times, poly $(A)^+$ RNA was isolated and subjected to northern blot analysis. The level of α-subunit mRNA (~9.4 kb) was quantified by a bioimage analyzer. Mean ± S.E.M. ($n = 3$).

Ca^{2+} channels without stimulating Na^+ influx (Yamamoto et al., 1997). In the present study, treatment with 20 mM LiCl for 24 h enhanced veratridine-induced $^{45}Ca^{2+}$ influx and catecholamine secretion by 33% and 30%, respectively (Fig. 8a and b; veratridine), whereas the same treatment did not alter high-K^+ (56 mM)-induced $^{45}Ca^{2+}$ influx and catecholamine secretion (Fig. 8a and b; high K^+).

4. Discussion

In the present study, we found that chronic treatment of adrenal chromaffin cells with LiCl increased cell surface density of $Na_V1.7$ Na^+ channels via accelerated Na^+ channel α-subunit gene transcription. In cells treated with LiCl, veratridine-induced $^{22}Na^+$ influx, subsequent $^{45}Ca^{2+}$ influx, and catecholamine secretion were augmented, whereas pharmacological and electrophysiological properties of Na^+ channels characterized by toxins (STX, veratridine, and PbTx-3) and patch-clamp analysis (Cestèle and Catterall, 2000) were similar to those of native Na^+ channels. These findings suggest that chronic lithium treatment up-regulates cell surface expression of native Na^+ channels via accelerated α-subunit gene transcription, resulting in enhanced Na^+ influx, subsequent Ca^{2+} influx and catecholamine secretion.

Increasing evidence has indicated that GSK-3 inhibition by lithium plays a crucial role in the metabolic, developmental, and neuronal effects of lithium (see reviews, Gurvich and Klein, 2002; Jope, 2003; Wada et al., 2005). Lithium inhibits GSK-3 activity (Ki = 1–2 mM) via two distinct mechanisms: direct inhibition of GSK-3 by competition for Mg^{2+} (Ryves and Harwood, 2001) and accumulation of Ser21/Ser9 phosphorylation of GSK-3α/-3β (Jope, 2003). In bovine adrenal chromaffin cells, we have demonstrated that LiCl increases Ser9 phosphorylation of GSK-3β and accumulation of β-catenin, a hallmark of GSK-3 inhibition (Yokoo et al., 2007; Nemoto et al., 2008). Inhibition of GSK-3β by LiCl or SB216763 decreases cell surface expression of insulin receptors by regulating mRNA levels (Yokoo et al., 2007). GSK-3β inhibition also decreases protein levels of insulin receptor substrate (IRS)-1, IRS-2, and Akt by regulating proteasomal degradation and/or synthesis (Nemoto et al., 2006, 2008). However, LiCl inhibited function of Na^+ channels independent of GSK-3 inhibition because other GSK-3 inhibitors (SB216763, SB415286 and GSK-3 inhibitor IX) did not inhibit the function of Na^+ channels and did not affect LiCl-induced inhibition of Na^+ channels (Yanagita et al., 2007). In the present study, LiCl, SB216763, and SB415286 up-regulated cell surface expression of Na^+ channels, whereas SB216763 and SB415286 did not have an additive effect on LiCl-induced up-regulation of Na^+ channels. In addition, we have previously reported that the anti-epileptic drug valproic acid, a potent inhibitor of GSK-3, also up-regulated cell surface expression of Na^+ channels (Yamamoto et al., 1997). Taken together, based on these previous and present studies, these results show that chronic lithium treatment up-regulates cell surface expression of Na^+ channels via inhibition of GSK-3β.

To avoid lithium intoxication, plasma lithium concentration must be strictly monitored. In patients with BPD, generally accepted therapeutic range of plasma lithium concentrations is 0.6–1.2 mmol/l, and toxic concentrations which cause neurotoxicity and nephrotoxicity begin above 1.5 mmol/l (Linder and Keck, 1998). Although these concentrations are about one order of magnitude lower than the concentration of LiCl (1–30 mM) that induced up-regulation of cell surface Na^+ channels in the present study, the concentrations used in the present study are comparable with those (1–20 mM) previously used in other in vitro studies that demonstrated various neuroprotective effects of lithium such as human neuroblastoma SH-SY5Y cells (De Sarno et al., 2002) and primary culture of cerebellar granule neurons (Jin et al., 2005). Moreover, we have previously reported that chronic (~24 h)

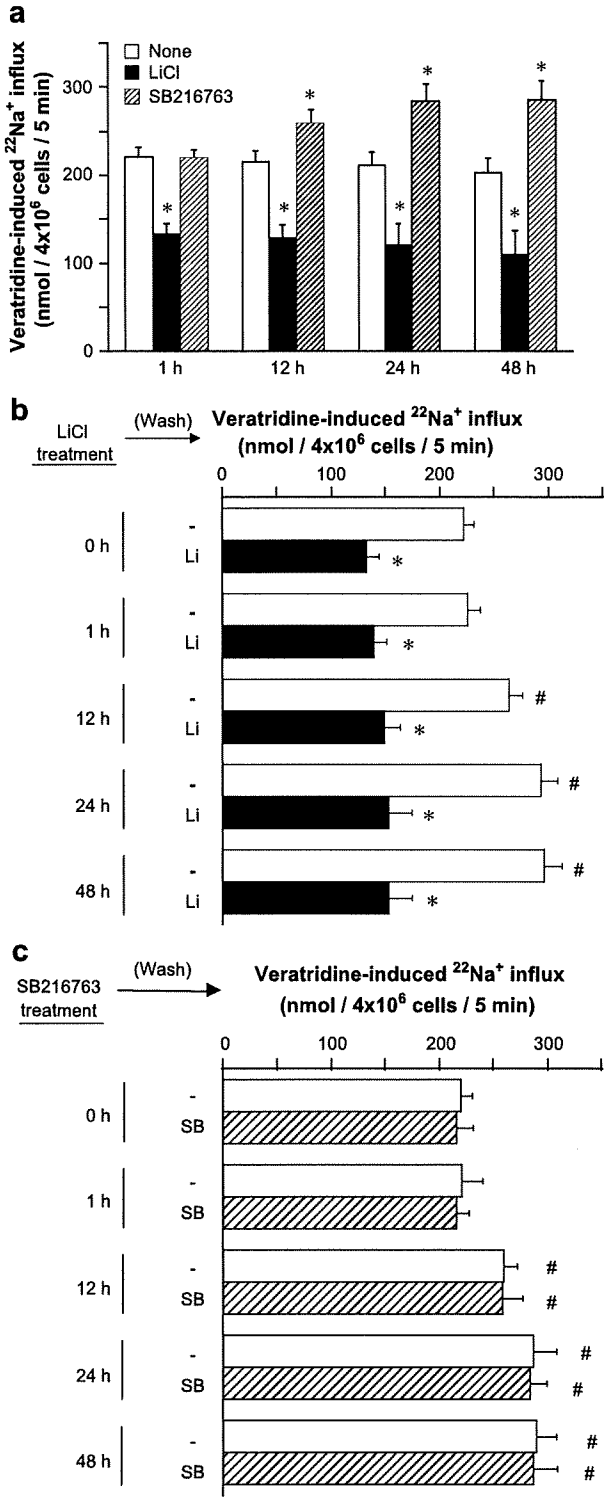

Fig. 5. Up-regulation of veratridine-induced $^{22}Na^+$ influx in cells chronically treated with LiCl and SB216763: inhibition by acute treatment with LiCl and increase by LiCl removal after chronic treatment. (a) Cells were treated with or without 20 mM LiCl or 10 μM SB216763 for up to 48 h. To examine the chronic effect of LiCl and SB216763 on $^{22}Na^+$ influx, at the end of the treatment periods (1, 12, 24, and 48 h), cells were exposed to 2 μCi $^{22}NaCl$ with or without 100 μM veratridine for an additional 5 min in the continuous presence or absence of 20 mM LiCl or 10 μM SB216763. Basal $^{22}Na^+$ influx values obtained at 37 °C without veratridine (nmol/4 × 10^6 cells/5 min) were not changed in cells treated with LiCl (1 h; 18.3 ± 1.8, 12 h; 18.8 ± 1.6, 24 h; 19.2 ± 1.7; 48 h; 18.9 ± 1.9) and SB216763 (1 h; 18.0 ± 1.7, 12 h; 18.2 ± 1.5, 24 h; 18.8 ± 1.9; 48 h; 18.3 ± 1.9) compared with untreated cells (1 h; 18.6 ± 1.6, 12 h; 18.6 ± 1.8, 24 h; 18.2 ± 1.8; 48 h; 17.8 ± 1.8). Basal values are subtracted from the data. Mean ± S.E.M. (n = 3). *P < 0.05, compared with nontreated cells. To examine the effect of removal of LiCl (b) or SB216763 (c) after chronic treatment on $^{22}Na^+$ influx, cells were treated with (1 h, 12 h, 24 h and 48 h) or without (None) 20 mM LiCl or 10 μM SB216763 for up to 48 h, washed with KRP buffer to remove LiCl or SB216763, and subjected to $^{22}Na^+$ influx. The cell groups were incubated with or without 100 μM veratridine for 5 min in KRP buffer containing 2 μCi $^{22}NaCl$ in the absence (−) or presence of 20 mM LiCl (Li) or 10 μM SB216763 (SB). Basal $^{22}Na^+$ influx values at 37 °C without veratridine were not changed and were subtracted from the data. Mean ± S.E.M. (n = 3). #P < 0.05, compared between nontreated cells (0 h) and LiCl- or SB216763-treated (1 h, 12 h, 24 h and 48 h) cells; *P < 0.05, compared with LiCl-nonexposed (−) cells within each time group.

treatment of bovine adrenal chromaffin cells with LiCl (0.1–30 mM) increased Ser9 phosphorylation of GSK-3β and accumulation of β-catenin without altering protein levels (Yokoo et al., 2007; Nemoto et al., 2008) and had no effect on cell viability (Yanagita et al., 2007), whereas 100 mM LiCl reduced cell viability by 45% in a time-dependent manner (Yanagita et al., 2007).

In addition to generating action potentials, Na^+ influx via Na^+ channels regulates the neuronal network from embryonic development through adulthood (e.g., differentiation into oligodendrocyte that myelinates axon, structural integrity of axons by heteroprotein assembly, development of neurites into a single axon and multiple dendrites, enhancement/opposition to attractive/repulsive molecules for axon growth cone navigation, correct synapse formation, epigenetic selection of neurotransmitter phenotype, experience-dependent cognition, neuronal survival, and axon remyelination) (Wada, 2006). In cultured dorsal root ganglion neurons, PC12 cells and NG108-15 cells, $Na_V1.7$ was localized predominantly to the axon growth cone (Toledo-Aral et al., 1997; Kawaguchi et al., 2007). Nerve growth factor (NGF) up-regulates $Na_V1.7$ in PC12 cells (D'Arcangelo et al., 1993) and NG108-15 cells (Kawaguchi et al., 2007) during neuronal differentiation. Interestingly, tightly regulated and localized inactivation of GSK-3β is essential for NGF-induced axon growth (Zhou et al., 2004). In the central and peripheral neurons, Ser9 phosphorylation of GSK-3β is required for neuronal polarization (Jiang et al., 2005; Yoshimura et al., 2006). Ser9-phosphorylated GSK-3β accumulates at the top of the axon in hippocampal neurons (Jiang et al., 2005) and dorsal root ganglion neurons (Zhou et al., 2004). Inhibition of GSK-3β by GSK-3 inhibitors (lithium, SB216763, or SB415286) induces formation of multiple axons, whereas overexpression of constitutively active GSK-3β inhibits axon formation (Jiang et al., 2005; Yoshimura et al., 2006). These correlative findings imply that up-regulation of $Na_V1.7$ and axon growth induced by GSK-3β inhibition may contribute to the neurotrophic/neuroprotective action of lithium. Lithium may have a disease-modifying benefit in the treatment of neurodegenerative disease via modulating axogenesis.

It has become clear that long-term changes in neuronal synaptic function are correlated with, and in some cases have been shown to be dependent on, the induction of new programs of gene expression (Hyman and Nestler, 1996). In the present study, LiCl increased the steady-state level of Na^+ channel α-subunit mRNA as early as 6 h, whereas [^{3}H]STX binding was increased at 12 h. The lithium-induced [^{3}H]STX binding increase was completely prevented by cycloheximide or actinomycin D. LiCl accelerated $Na_V1.7$ α-subunit gene transcription without altering α-subunit mRNA stability. These results suggest that chronic LiCl treatment accelerates α-subunit gene transcription, thus leading to the increased steady-state level of α-subunit mRNA and the increased cell surface expression of Na^+ channels. Recently, the promoter region of the $Na_V1.7$ Na^+ channel gene (SCN9A) has been identified, and it contains binding elements for the transcription factors Sp1, egr1, Brn3, and repressor element silencing transcription/neuron-restrictive silencer factor (REST/NRSF) (Diss et al., 2008).

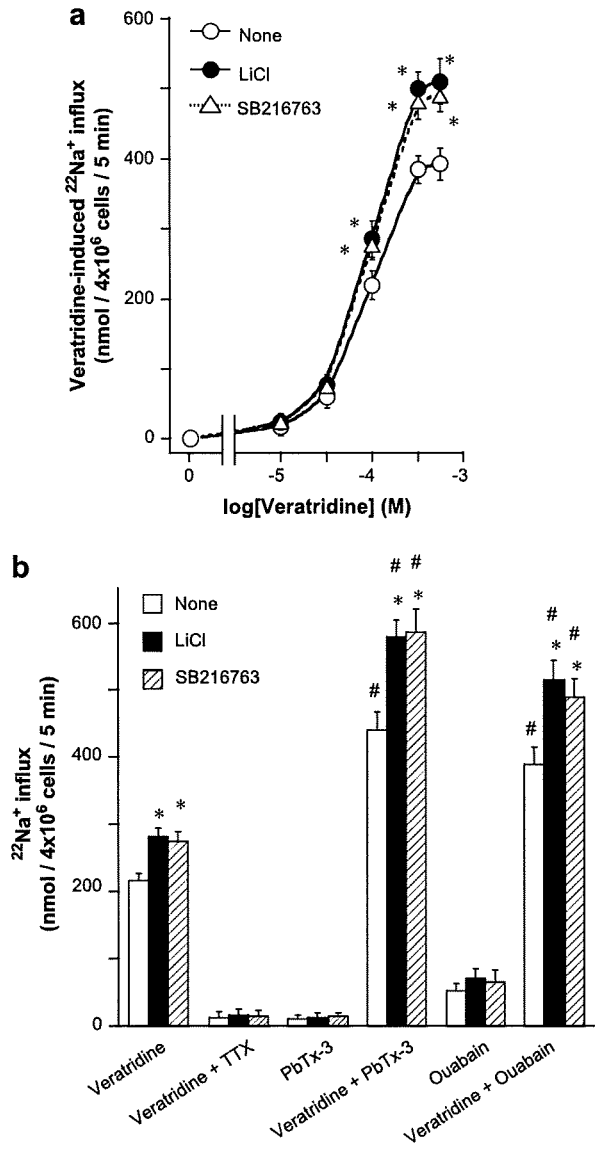

Fig. 6. Effect of chronic LiCl or SB216763 treatment on $^{22}Na^+$ influx measured in the presence and absence of veratridine, TTX, PbTx-3, and ouabain. Cells were treated with or without 20 mM LiCl or 10 μM SB216763 for 24 h and washed with KRP buffer, then exposed to 2 μCi $^{22}NaCl$ for 5 min in the presence or absence of (a) 1–500 μM veratridine, or (b) 100 μM ouabain, 100 μM veratridine and/or 1 μM PbTx-3. Basal $^{22}Na^+$ influx value at 37 °C (nmol/4 × 10^6 cells/5 min) was not changed in cells treated with LiCl (19.2 ± 1.7) or SB216763 (18.8 ± 2.0) relative to untreated cells (18.6 ± 1.9). These basal values are subtracted from the data. Mean ± S.E.M. (n = 3). *P < 0.05, compared with LiCl-untreated cells; #P < 0.05, compared with veratridine alone within each untreated and LiCl-treated cell group.

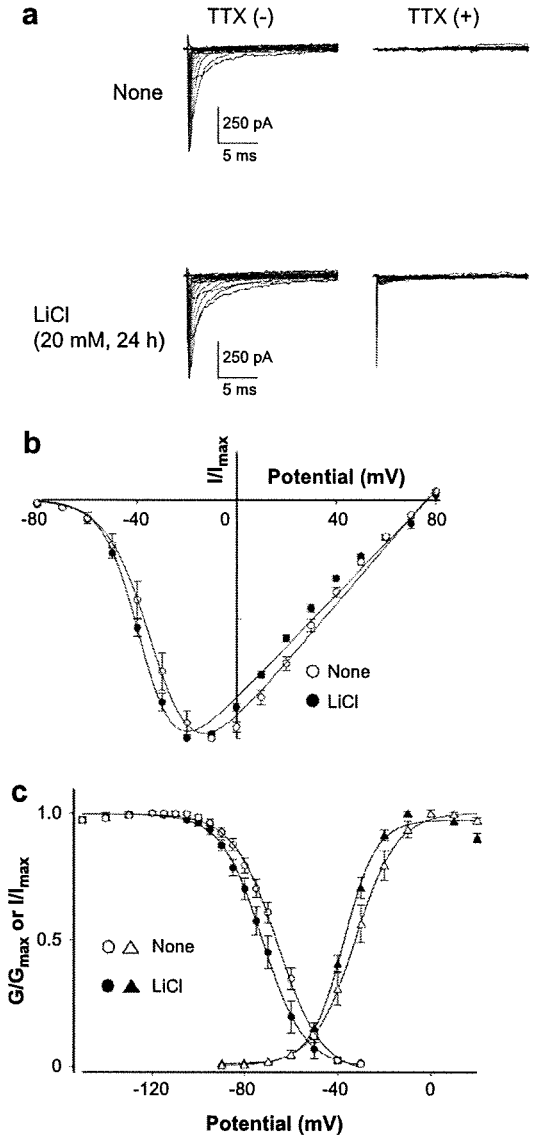

Fig. 7. Whole-cell patch-clamp analysis: similar electrophysiological properties between untreated and LiCl-treated cells. Cells were treated with or without 20 mM LiCl for 24 h, washed, and subjected to whole cell patch-clamp analysis in the absence of LiCl. (a) Representative Na^+ current traces were recorded in the presence or absence of 1 μM TTX. Currents were elicited by voltage steps in 10 mM increments from −90 mV to 90 mV from a holding potential of −120 mV. (b) Normalized I–V relation in cells pretreated with or without 20 mM LiCl for 24 h. (c) Voltage-dependence of steady-state inactivation (circle) and activation (triangle) in cells pretreated without (open circle or triangle) or with (closed circle or triangle) 20 mM LiCl for 24 h. Mean ± S.E.M. (n = 10).

Among these transcription factors, REST/NRSF has been reported to be modulated by lithium: in cultured rat neural stem cells, lithium reduces DNA binding activity of REST/NRSF and increases neuronal differentiation (Ishii et al., 2008). REST/NRSF is identified as a factor that influences the expression of brain type $Na_V1.2$ Na^+ channels (Chong et al., 1995). REST/NRSF suppresses multiple neuronal target genes (e.g., $Na_V1.2$, SCG10, synapsin I, and glutamate receptor) in undifferentiated neural precursors, and down-regulation of REST/NRSF during neurogenesis is required for proper development and for the acquisition of the terminally differentiated phenotype (Ballas et al., 2001; Ishii et al., 2008). These correlative findings imply that reduced DNA binding activity of REST/NRSF caused by lithium might be involved in the acceleration of $Na_V1.7$ α-subunit gene transcription, although the precise mechanism has yet to be identified.

Despite compelling evidence of the long-term therapeutic effects of lithium, sudden cessation of lithium therapy causes the rapid return of manic symptoms (Baldessarini et al., 1999). This rebound mania is not a simple reemergence of the original disorder, but appears to be a worsening of the condition, with patients being at higher risk of suffering a manic episode than would be predicted by the natural history of the disease (Baldessarini et al., 1999), and

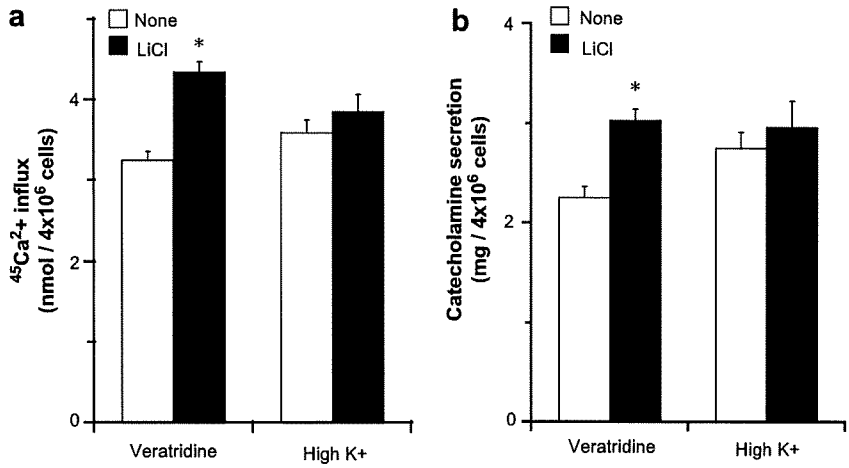

Fig. 8. Up-regulation of veratridine- (but not high K^+-) induced (a) $^{45}Ca^{2+}$ influx and (b) catecholamine secretion in cells treated with LiCl. Cells treated for 24 h with (closed columns) or without (open columns) 20 mM LiCl were washed and then incubated with 2 μCi $^{45}CaCl_2$ at 37 °C in the presence or absence of 100 μM veratridine for 5 min in KRP buffer, or in 56 mM high K^+ solution for 1 min. Basal values obtained at 37 °C without veratridine or high K^+ were not changed by LiCl treatment and were subtracted from the data. Mean ± SE ($n = 3$). *$P < 0.05$, compared with LiCl-untreated cells.

the mechanisms precipitating this rebound mania are unclear. In the present study, in cells chronically treated with LiCl, LiCl also inhibited veratridine-induced $^{22}Na^+$ influx in a way similar to untreated cells (Yanagita et al., 2007). However, removal of LiCl after chronic treatment enhanced veratridine-induced $^{22}Na^+$ influx, $^{45}Ca^{2+}$ influx and catecholamine secretion due to LiCl-induced up-regulation of Na^+ channels. This enhancement of Na^+ influx, and subsequent Ca^{2+} channel gating and catecholamine secretion induced by withdrawal from chronic lithium treatment, may provide insight into the mechanism of rebound mania. Randomized clinical trials have shown that Na^+ channel-inhibiting antiepileptic drugs (e.g., valproic acid, lamotrigine, riluzole, phenytoin, and carbamazepine) are effective in treating BPD (Rogawski and Loscher, 2004). These antiepileptic drugs have no direct effects on receptors or neurotransmitters (Stoll and Severus, 1996), but indirectly and nonspecifically inhibit neurotransmitter release via their primary effect on presynaptic Na^+ channel blockade (Rogawski and Loscher, 2004; Askland, 2006). Furthermore, development of resistance to antiepileptic drugs observed in the treatment for BPD derives from the loss of Na^+ channel inhibition (Remy and Beck, 2006). A simple interpretation of these correlative findings is that Na^+ channel function modulated by therapeutic drugs may directly affect aberrant neuronal excitability in BPD patients, thus enhancement of Na^+ influx caused by lithium withdrawal may trigger recurrence of mania. Further in vivo and in vitro investigations are required to elucidate the relationship between lithium withdrawal-induced enhancement of Na^+ influx through brain type Na^+ channels ($Na_V1.1$–1.3) and rebound mania.

In conclusion, chronic treatment with lithium up-regulates cell surface expression of native $Na_V1.7$ Na^+ channels via GSK-3 inhibition in cultured bovine adrenal chromaffin cells. Withdrawal from chronic lithium treatment enhances Na^+ influx and subsequent Ca^{2+} channel gating and catecholamine secretion in response to up-regulation of cell surface Na^+ channels. The present findings provide insight into the pharmacotherapy of BPD and neurodegenerative diseases.

Acknowledgments

We thank Drs. Franz Hofmann and Youngsuk Oh for donating hNE-Na and β_1-subunit plasmids, respectively. Technical and secretarial assistance by Ms. Keiko Kawabata, Ms. Masako Yamamoto, and Ms. Naoko Tokashiki is appreciated. This study was supported in part by a Grant-in-Aid for The 21st Century COE (Centers of Excellence) Program (Life Science) and by a Grant-in-Aid for The Scientific Research (B) (to AW 30131949), Scientific Research (C) (to TY 60295227), and Young Scientists (A) (to TY 60295227), from the Ministry of Education, Culture, Sports, Science and Technology, Japan.

References

Askland, K., 2006. Toward a biaxial model of "bipolar" affective disorders: further exploration of genetic, molecular and cellular substrates. J. Affect Disord. 94, 35–66.

Baldessarini, R.J., Tondo, L., Viguera, A.C., 1999. Discontinuing lithium maintenance treatment in bipolar disorders: risks and implications. Bipolar. Disord. 1, 17–24.

Ballas, N., Battaglioli, E., Atouf, F., Andres, M.E., Chenoweth, J., Anderson, M.E., Burger, C., Moniwa, M., Davie, J.R., Bowers, W.J., Federoff, H.J., Rose, D.W., Rosenfeld, M.G., Brehm, P., Mandel, G., 2001. Regulation of neuronal traits by a novel transcriptional complex. Neuron 31, 353–365.

Catterall, W.A., 2000. From ionic currents to molecular mechanisms: the structure and function of voltage-gated sodium channels. Neuron 26, 13–25.

Cestèle, S., Catterall, W.A., 2000. Molecular mechanisms of neurotoxin action on voltage-gated sodium channels. Biochimie 82, 883–892.

Coghlan, M.P., Culbert, A.A., Cross, D.A., Corcoran, S.L., Yates, J.W., Pearce, N.J., Rausch, O.L., Murphy, G.J., Carter, P.S., Roxbee, Cox.L., Mills, D., Brown, M.J., Haigh, D., Ward, R.W., Smith, D.G., Murray, K.J., Reith, A.D., Holder, J.C., 2000. Selective small molecule inhibitors of glycogen synthase kinase-3 modulate glycogen metabolism and gene transcription. Chem. Biol. 7, 793–803.

Chong, J.A., Tapia-Ramírez, J., Kim, S., Toledo-Aral, J.J., Zheng, Y., Boutros, M.C., Altshuller, Y.M., Frohman, M.A., Kraner, S.D., Mandel, G., 1995. REST: a mammalian silencer protein that restricts sodium channel gene expression to neurons. Cell 80, 949–957.

D'Arcangelo, G., Paradiso, K., Shepherd, D., Brehm, P., Halegoua, S., 1993. Neuronal growth factor regulation of two different sodium channel types through distinct signal transduction pathways. J. Cell Biol. 122, 915–921.

De Sarno, P., Li, X., Jope, R.S., 2002. Regulation of Akt and glycogen synthase kinase-3β phosphorylation by sodium valproate and lithium. Neuropharmacology 43, 1158–1164.

Diss, J.K., Calissano, M., Gascoyne, D., Djamgoz, M.B., Latchman, D.S., 2008. Identification and characterization of the promoter region of the Nav1.7 voltage-gated sodium channel gene (SCN9A). Mol. Cell Neurosci. 37, 537–547.

Gurvich, N., Klein, P.S., 2002. Lithium and valproic acid: parallels and contrasts in diverse signaling contexts. Pharmacol. Ther. 96, 45–66.

Hamill, O.P., Marty, A., Neher, E., Sakmann, B., Sigworth, F.J., 1981. Improved patch-clamp techniques for high-resolution current recording from cells and cell-free membrane patches. Pflugers Arch. 3912, 85–100.

Hyman, S.E., Nestler, E.J., 1996. Initiation and adaptation: a paradigm for understanding psychotropic drug action. Am. J. Psychiatry 153, 151–162.

Ishii, T., Hashimoto, E., Ukai, W., Tateno, M., Yoshinaga, T., Saito, S., Sohma, H., Saito, T., 2008. Lithium-induced suppression of transcription repressor NRSF/

REST: effects on the dysfunction of neuronal differentiation by ethanol. Eur. J. Pharmacol. 593, 36–43.
Jiang, H., Guo, W., Liang, X., Rao, Y., 2005. Both the establishment and the maintenance of neuronal polarity require active mechanisms: critical roles of GSK-3β and its upstream regulators. Cell 120, 123–135.
Jin, N., Kovacs, A.D., Sui, Z., Dewhurst, S., Maggirwar, S.B., 2005. Opposite effects of lithium and valproic acid on trophic factor deprivation-induced glycogen synthase kinase-3 activation, c-Jun expression and neuronal cell death. Neuropharmacology 48, 576–583.
Jope, R.S., 2003. Lithium and GSK-3: one inhibitor, two inhibitory actions, multiple outcomes. Trends Pharmacol. Sci. 24, 441–443.
Kawaguchi, A., Asano, H., Matsushima, K., Wada, T., Yoshida, S., Ichida, S., 2007. Enhancement of sodium current in NG108-15 cells during neural differentiation is mainly due to an increase in NaV1.7 expression. Neurochem. Res. 32, 1469–1475.
Klugbauer, N., Lacinova, L., Flockerzi, V., Hofmann, F., 1995. Structure and functional expression of a new member of the tetrodotoxin-sensitive voltage-activated sodium channel family from human neuroendocrine cells. EMBO J. 14, 1084–1090.
Linder, M.W., Keck Jr., P.E., 1998. Standards of laboratory practice: antidepressant drug monitoring. National Academy of Clinical Biochemistry. Clin. Chem. 44, 1073–1084.
Linsdell, P., Moody, W.J., 1994. Na^+ channel mis-expression accelerates K^+ channel development in embryonic *Xenopus laevis* skeletal muscle. J. Physiol. (Lond.) 480, 405–410.
Maruta, T., Yanagita, T., Matsuo, K., Uezono, Y., Satoh, S., Nemoto, T., Yoshikawa, N., Kobayashi, H., Takasaki, M., Wada, A., 2008. Lysophosphatidic acid-LPA1 receptor-Rho-Rho kinase-induced up-regulation of $Na_V1.7$ sodium channel mRNA and protein in adrenal chromaffin cells: enhancement of $^{22}Na^+$ influx, $^{45}Ca^{2+}$ influx and catecholamine secretion. J. Neurochem. 105, 401–412.
Nemoto, T., Kanai, T., Yanagita, T., Satoh, S., Maruta, T., Yoshikawa, N., Kobayashi, H., Wada, A., 2008. Regulation of Akt mRNA and protein levels by glycogen synthase kinase-3β in adrenal chromaffin cells: effects of LiCl and SB216763. Eur. J. Pharmacol. 586, 82–89.
Nemoto, T., Yokoo, H., Satoh, S., Yanagita, T., Sugano, T., Yoshikawa, N., Maruta, T., Kobayashi, H., Wada, A., 2006. Constitutive activity of glycogen synthase kinase-3β: positive regulation of steady-state levels of insulin receptor substrates-1 and -2 in adrenal chromaffin cells. Brain Res. 1110, 1–12.
Oh, Y., Waxman, S.G., 1994. The β_1-subunit mRNA of the rat brain Na^+ channel is expressed in glial cells. Proc. Natl. Acad. Sci. U.S.A. 91, 9985–9989.
Remy, S., Beck, H., 2006. Molecular and cellular mechanisms of pharmacoresistance in epilepsy. Brain 129, 18–35.
Rogawski, M.A., Loscher, W., 2004. The neurobiology of antiepileptic drugs for the treatment of nonepileptic conditions. Nat. Med. 10, 685–692.
Ryves, W.J., Harwood, A.J., 2001. Lithium inhibits glycogen synthase kinase-3 by competition for magnesium. Biochem. Biophys. Res. Commun. 280, 720–725.
Stoll, A.L., Severus, W.E., 1996. Mood stabilizers: shared mechanisms of action at postsynaptic signal-transduction and kindling processes. Harv. Rev. Psychiatry 4, 77–89.
Toledo-Aral, J.J., Moss, B.L., He, Z-J., Koszowski, A.G., Whisenand, T., Levinson, S.R., Wolf, J.J., Silos-Santiago, I., Halegoua, S., Mandel, G., 1997. Identification of PN1, a predominant voltage-dependent sodium channel expressed principally in peripheral neurons. Proc. Natl. Acad. Sci. USA 94, 1527–1532.
Wada, A., 2006. Roles of voltage-dependent sodium channels in neuronal development, pain, and neurodegeneration. J. Pharm. Sci. 102, 253–268.
Wada, A., Yanagita, T., Yokoo, H., Kobayashi, H., 2004. Regulation of cell surface expression of voltage-dependent $Na_V1.7$ sodium channels: mRNA stability and posttranscriptional control in adrenal chromaffin cells. Front. Biosci. 9, 1954–1966.
Wada, A., Yokoo, H., Yanagita, T., Kobayashi, H., 2005. Lithium: potential therapeutics against acute brain injuries and chronic neurodegenerative diseases. J. Pharmacol. Sci. 99, 307–321.
Waxman, S.G., Dib-Hajj, S., Cummins, T.R., Black, J.A., 2000. Sodium channels and their genes: dynamic expression in the normal nervous system, dysregulation in disease states. Brain Res. 886, 5–14.
Yamamoto, R., Yanagita, T., Kobayashi, H., Yokoo, H., Wada, A., 1997. Up-regulation of sodium channel subunit mRNAs and their cell surface expression by antiepileptic valproic acid: activation of calcium channel and catecholamine secretion in adrenal chromaffin cells. J. Neurochem. 68, 1655–1662.
Yanagita, T., Kobayashi, H., Yamamoto, R., Kataoka, H., Yokoo, H., Shiraishi, S., Minami, S., Koono, M., Wada, A., 2000. Protein kinase C-α and -ε down regulate cell surface sodium channels via differential mechanisms in adrenal chromaffin cells. J. Neurochem. 74, 1674–1684.
Yanagita, T., Kobayashi, H., Uezono, Y., Yokoo, H., Sugano, T., Saitoh, T., Minami, S., Shiraishi, S., Wada, A., 2003. Destabilization of $Na_V1.7$ sodium channel α-subunit mRNA by constitutive phosphorylation of extracellular signal-regulated kinase: negative regulation of steady-state level of cell surface functional sodium channels in adrenal chromaffin cells. Mol. Pharmacol. 63, 1125–1136.
Yanagita, T., Kobayashi, H., Uezono, Y., Yokoo, H., Sugano, T., Saitoh, T., Minami, S., Shiraishi, S., Wada, A., 2007. Lithium inhibits function of voltage-dependent sodium channels and catecholamine secretion independent of glycogen synthase kinase-3 in adrenal chromaffin cells. Neuropharmacology 53, 881–889.
Yokoo, H., Nemoto, T., Yanagita, T., Satoh, S., Yoshikawa, N., Maruta, T., Wada, A., 2007. Glycogen synthase kinase-3β: homologous regulation of cell surface insulin receptor level via controlling insulin receptor mRNA stability in adrenal chromaffin cells. J. Neurochem. 103, 1883–1896.
Yoshimura, T., Arimura, N., Kaibuchi, K., 2006. Signaling networks in neuronal polarization. J. Neurosci. 26, 10626–10630.
Zhou, F.Q., Zhou, J., Dedhar, S., Wu, Y.H., Snider, W.D., 2004. NGF-induced axon growth is mediated by localized inactivation of GSK-3beta and functions of the microtubule plus end binding protein APC. Neuron 426, 897–912.